infection who received rituximab plus steroids containing chemotherapy.[15] The kinetics of HBV reactivation in this case strongly suggested that monthly monitoring of HBV DNA could prevent hepatitis even in such a highly replicative clone with a precore mutation.

In summary, we first reported HBV reactivation following treatment with the anti-CCR4 antibody mogamulizumab and revealed the detailed kinetics of HBV replication during reactivation. Further well-designed studies are warranted to address the mechanisms of HBV reactivation and to establish standard management for reactivation in patients with previously resolved HBV infection, following anticancer chemotherapy and immunosuppressive therapy.

## ACKNOWLEDGMENTS

THIS STUDY WAS supported in part by the Ministry of Health, Labour and Welfare of Japan (Grant-in-Aid H24-kanen-004 to M. M.) and the Ministry of Education, Culture, Sports Science and Technology of Japan (Grant-in-Aid for Scientific Research (C) no. 90423855 to S. K.) and Grant-in-Aid for National Cancer Center Research and Development Fund (no. 23-A-17 to T. I.).

## REFERENCES

1 Lok AS, Liang RH, Chiu EK *et al.* Reactivation of hepatitis B virus replication in patients receiving cytotoxic therapy. Report of a prospective study. *Gastroenterology* 1991; **100**: 182–8.
2 Dervite I, Hober D, Morel P. Acute hepatitis B in a patient with antibodies to hepatitis B surface antigen who was receiving rituximab. *N Engl J Med* 2001; **344**: 68–9.
3 Hui CK, Cheung WW, Zhang HY *et al.* Kinetics and risk of de novo hepatitis B infection in HBsAg-negative patients undergoing cytotoxic chemotherapy. *Gastroenterology* 2006; **131**: 59–68.
4 Yeo W, Chan TC, Leung NW *et al.* Hepatitis B virus reactivation in lymphoma patients with prior resolved hepatitis B undergoing anticancer therapy with or without rituximab. *J Clin Oncol* 2009; **27**: 605–11.
5 Kusumoto S, Tanaka Y, Mizokami M *et al.* Reactivation of hepatitis B virus following systemic chemotherapy for malignant lymphoma. *Int J Hematol* 2009; **90**: 13–23.
6 Matsue K, Kimura S, Takanashi Y *et al.* Reactivation of hepatitis B virus after rituximab-containing treatment in patients with CD20-positive B-cell lymphoma. *Cancer* 2010; **116**: 4769–76.
7 Ishida T, Ueda R. Antibody therapy for Adult T-cell leukemia-lymphoma. *Int J Hematol* 2011; **94**: 443–52.
8 Ishii T, Ishida T, Utsunomiya A *et al.* Defucosylated humanized anti-CCR4 monoclonal antibody KW-0761 as a novel immunotherapeutic agent for adult T-cell leukemia/lymphoma. *Clin Cancer Res* 2010; **16**: 1520–31.
9 Yamamoto K, Utsunomiya A, Tobinai K *et al.* Phase I study of KW-0761, a defucosylated humanized anti-CCR4 antibody, in relapsed patients with adult T-cell leukemia-lymphoma and peripheral T-cell lymphoma. *J Clin Oncol* 2010; **28**: 1591–8.
10 Ishida T, Joh T, Uike N *et al.* Defucosylated anti-CCR4 monoclonal antibody (KW-0761) for relapsed adult T-cell leukemia-lymphoma: a multicenter phase II study. *J Clin Oncol* 2012; **30**: 837–42.
11 Sugawara K, Nakayama N, Mochida S. Acute liver failure in Japan: definition, classification, and prediction of the outcome. *J Gastroenterol* 2012; **47**: 849–61.
12 Oketani M, Ido A, Nakayama N *et al.* Etiology and prognosis of fulminant hepatitis and late-onset hepatic failure in Japan: summary of the annual nationwide survey between 2004 and 2009. *Hepatol Res* 2013; **43**: 97–105.
13 Oketani M, Ido A, Uto H *et al.* Prevention of hepatitis B virus reactivation in patients receiving immunosuppressive therapy or chemotherapy. *Hepatol Res* 2012; **42**: 627–36.
14 European Association For The Study Of The Liver. EASL clinical practice guidelines: management of chronic hepatitis B virus infection. *J Hepatol* 2012; **57**: 167–85.
15 Kusumoto S, Tanaka Y, Suzuki R *et al.* Prospective nationwide observational study of hepatitis B virus (HBV) DNA monitoring and preemptive antiviral therapy for HBV reactivation in patients with B-cell non-Hodgkin lymphoma following rituximab containing chemotherapy: results of interim analysis. *Blood* 2012; **120**: abstract 2641.

EUROPEAN JOURNAL OF Haematology

European Journal of Haematology 92 (219–228)

ORIGINAL ARTICLE

# Antitumor effects of bevacizumab in a microenvironment-dependent human adult T-cell leukemia/lymphoma mouse model

Fumiko Mori[1], Takashi Ishida[1], Asahi Ito[1], Fumihiko Sato[2], Ayako Masaki[1], Tomoko Narita[1], Susumu Suzuki[2], Tomiko Yamada[1], Hisashi Takino[2], Masaki Ri[1], Shigeru Kusumoto[1], Hirokazu Komatsu[1], Masakatsu Hishizawa[3], Kazunori Imada[4], Akifumi Takaori-Kondo[3], Akio Niimi[1], Ryuzo Ueda[5], Hiroshi Inagaki[2], Shinsuke Iida[1]

[1]Department of Medical Oncology and Immunology, Nagoya City University Graduate School of Medical Sciences, Nagoya;[2]Department of Anatomic Pathology and Molecular Diagnostics, Nagoya City University Graduate School of Medical Sciences, Nagoya; [3]Department of Hematology and Oncology, Graduate School of Medicine, Kyoto University, Kyoto; [4]Department of Hematology, Kokura Memorial Hospital, Kitakyushu; [5]Department of Tumor Immunology, Aichi Medical University School of Medicine, Nagakute, Japan

## Abstract

*Objective:* The objective of this study was to evaluate the therapeutic potential of bevacizumab with or without systemic chemotherapy for adult T-cell leukemia/lymphoma (ATL) and clarify the significance of angiogenesis for ATL pathogenesis. *Methods:* NOD/Shi-*scid*, IL-2R$\gamma^{null}$ (NOG) mice were used as recipients of tumor cells from a patient with ATL, which engraft and proliferate in a microenvironment-dependent manner. The ATL cells could be serially transplanted in NOG mice, but could not be maintained in *in vitro* cultures. *Results:* Injection of bevacizumab alone significantly increased necrosis and decreased vascularization in the tumor tissue. Levels of human soluble interleukin two receptor in the serum (reflecting the ATL tumor burden) of bevacizumab-treated mice were significantly lower than in untreated mice. Although bevacizumab monotherapy showed these clear anti-angiogenesis effects, it did not prolong survival. In contrast, injection of bevacizumab together with cyclophosphamide, doxorubicin, vincristine, prednisolone (CHOP) led to a significant prolongation of survival of the ATL mice relative to CHOP alone. *Conclusions:* This is the first report to evaluate the efficacy of bevacizumab for ATL in a tumor microenvironment-dependent model. Bevacizumab therapy combined with chemotherapy could be a valuable treatment strategy for that subgroup of ATL probably depending to a large extent on angiogenesis via vascular endothelial growth factor.

**Key words** Adult T-cell leukemia-lymphoma; Bevacizumab; tumor microenvironment

**Correspondence** Takashi Ishida, MD, PhD, Department of Medical Oncology and Immunology, Nagoya City University Graduate School of Medical Sciences, 1 Kawasumi, Mizuho-chou, Mizuho-ku, Nagoya, Aichi 467-8601, Japan. Tel: +81 52 853 8216; Fax: +81 52 852 0849; e-mail: itakashi@med.nagoya-cu.ac.jp

Accepted for publication 29 October 2013

doi:10.1111/ejh.12231

Adult T-cell leukemia-lymphoma (ATL) is an aggressive peripheral T-cell neoplasm caused by human T-cell lymphotropic virus type 1 (HTLV-1). The disease is resistant to conventional chemotherapeutic agents, and currently there are only limited treatment options; thus, it has a very poor prognosis (1–4). Over the past decade, allogeneic hematopoietic stem-cell transplantation has evolved into a potential approach to treating patients with ATL. However, only a small fraction of patients have the opportunity to benefit from transplantation, such as those who are younger, have achieved sufficient disease control, and have an appropriate stem-cell source (5, 6). Therefore, the development of alternative treatment strategies for patients with ATL is an urgent issue.

Bevacizumab is a humanized monoclonal antibody against the vascular endothelial growth factor A (VEGF-A), a key

factor inducing the formation of blood vessels (angiogenesis) in tumors (7). Bevacizumab is currently approved worldwide for the treatment of several types of cancer such as metastatic colorectal cancer, metastatic non-small-cell lung cancer, renal cell carcinoma, and advanced ovarian cancer, in combination with chemotherapy or interferon (8–14). Bevacizumab is also approved as a single agent for recurrent glioblastoma in the USA (15). In this context, many aspects of pathological angiogenesis have been extensively studied in many types of cancer. On the other hand, the precise role of these processes in pathogenesis of hematological malignancies including ATL is still under active investigation (16–19). Thus far, bevacizumab has not been approved for the treatment of any hematological malignancy in the USA, Europe, or Japan. The aim of the present study was to evaluate the therapeutic potential of bevacizumab with or without systemic chemotherapy for ATL and clarify the significance of angiogenesis for ATL pathogenesis, using a microenvironment-dependent murine ATL model.

## Methods

### Animals

NOD/Shi-*scid*, IL-2R$\gamma^{null}$ (NOG) mice (20) were purchased from the Central Institute for Experimental Animals (Kanagawa, Japan) and used at 6–8 wk of age. All of the *in vivo* experiments were performed in accordance with the United Kingdom Coordinating Committee on Cancer Research Guidelines for the Welfare of Animals in Experimental Neoplasia, Second Edition, and were approved by the Ethics Committee of the Center for Experimental Animal Science, Nagoya City University Graduate School of Medical Sciences.

### Immunopathological analysis

We assessed the affected lymph nodes of 23 patients with ATL by immunopathology. The patients provided written informed consent in accordance with the Declaration of Helsinki, and this present study was approved by the institutional Ethics Committee of Nagoya City University Graduate School of Medical Sciences. Hematoxylin and eosin (HE) staining and immunostaining using anti-human CD4 (4B12; Novocastra, Wetzlar, Germany), CD25 (4C9; Novocastra), CD20 (L26; DAKO, Glostrup, Denmark), VEGF-A (sc-152, rabbit polyclonal; Santa Cruz, Heidelberg, Germany), Alpha-Smooth Muscle Actin (α-SMA) (1A4; DAKO), CD31 (JC70A; DAKO), and von Willebrand Factor (Rabbit polyclonal; DAKO) were performed on formalin-fixed, paraffin-embedded sections. VEGF-A expression levels were categorized according to the following formula: 3+ positive if ≥50%, 2+ positive if <50 ≥30%, 1+ positive if <30 ≥10%, and negative if <10% of the ATL tumor cells were stained with the corresponding antibody. Nine 100× high-power fields (HPF) of HE tumor specimens were randomly selected, and the area of tumor necrosis (%) was calculated by Image J software (21), and then averaged. Nine 100× HPF of von Willebrand Factor-stained tumor specimens were randomly selected, and numbers of vessels (per $mm^2$) were calculated by Image J software and then averaged.

### ATL mouse model

A leukemic cell clone from a patient with ATL, which could be serially transplanted into SCID mice, designated S-YU as reported previously (22), was injected intraperitoneally (i.p.) into NOG mice. Three to 4 wk after i.p. injection, NOG mice were presented with intraperitoneal masses along the mesentery. Cells from these intraperitoneal masses were suspended in RPMI-1640 and inoculated i.p. into healthy NOG mice, which then presented with features identical to those of the original mice.

### Cell lines

ATN-1, MT-1, and TL-Om1 are ATL cell lines, whereas MT-2, MT-4, and TL-Su are HTLV-1-immortalized lines, as previously described (23).

### Quantitative reverse transcription-polymerase chain reaction

Total RNA was isolated with RNeasy Mini Kits (QIAGEN, Tokyo, Japan). Reverse transcription from the RNA to first strand cDNA was carried out using High Capacity RNA-to-cDNA Kits (Applied Biosystems Inc, Foster City, CA, USA). *Human VEGF-A* (Hs00900055_m1), *VEGF-R1* (Hs00176573_m1), *VEGF-R2* (Hs00911700_m1), and *β-actin* (Hs99999903_m1) *mRNA* were amplified using TaqMan® Gene Expression Assays with the aid of an Applied Biosystems StepOnePlus™. The quantitative assessment of the mRNA of interest was done by dividing its level by that of *β-actin* and expressing the result relative to Human Testis Total RNA (Clontech, Mountain View, CA, USA) as 1.0. All expressed values were averages of triplicate experiments.

### Monoclonal antibodies and flow cytometry

The following Monoclonal antibodies (mAbs) were used for flow cytometry: APC-conjugated anti-human CD45 mAb (2D1; BD Biosciences, San Jose, CA, USA), PerCP-conjugated anti-CD4 mAb (SK3; BD Biosciences), PE-conjugated anti-CD25 mAb (M-A251; BD Biosciences), PE-conjugated VEGF-R1 mAb (49560; BD Biosciences), PE-conjugated VEGF-R2 mAb (89106, R&D Systems, Inc. Minneapolis, MN,

USA), and the appropriate isotype control mAbs. Whole blood was treated with BD FACS lysing solution (BD Biosciences) to remove RBC. Stained cells were analyzed on a FACSCalibur (BD Biosciences) with the aid of FlowJo software (Tree Star, Inc. Ashland, OR, USA).

### Cell proliferation assay

Proliferation of S-YU and HTLV-I-immortalized lines expressing both VEGF-A and VEGF-R1 in the presence of different concentrations of bevacizumab for 48 h was assessed using CellTiter 96 Aqueous One Solution cell proliferation assay kits (Promega Corporation, Madison, WI, USA). Bevacizumab was purchased from Chugai Pharmaceutical Co., Ltd., Tokyo, Japan.

### ATL cell-bearing mice treated with bevacizumab

ATL tumor cells (S-YU) from the intraperitoneal masses were suspended in RPMI-1640, and $1.0 \times 10^7$ was inoculated i.p. into each of 14 NOG mice. The animals were divided into two groups of seven each for treatment with bevacizumab or to serve as controls. Bevacizumab (10 mg/kg) or vehicle (saline) was i.p. injected into the mice 3, 10, and 17 d after tumor cell inoculations. Therapeutic efficacies were evaluated for area of tumor necrosis, number of vessels, and serum human sIL2R levels 22 d after tumor inoculation. The concentration of human sIL2R in the serum was measured by ELISA using human sIL2R immunoassay kits (R&D Systems, Inc.).

ATL cells from the intraperitoneal masses suspended in RPMI-1640 were also inoculated i.p. into another 10 NOG mice at $1.0 \times 10^7$ per mouse. These animals were randomly divided into two groups of five each for treatment with bevacizumab or as controls. Bevacizumab (10 mg/kg) or saline was injected i.p. into the mice 2, 9, 16, and 23 d after tumor cell inoculation. Therapeutic efficacy of bevacizumab was evaluated by survival times.

A further 16 NOG mice that had also received $1.0 \times 10^7$ ATL cells from intraperitoneal masses were randomly divided into two groups of eight each for treatment with bevacizumab + cyclophosphamide, doxorubicin, vincristine, prednisolone (CHOP) or CHOP alone. Bevacizumab (10 mg/kg) or saline was i.p. injected into the mice 2, 9, 16, 23, 30, and 37 d after tumor cell inoculations. CHOP was given i.p. 17 d after tumor inoculation at the following doses: cyclophosphamide, 40 mg/kg; doxorubicin, 3.3 mg/kg; vincristine, 0.5 mg/kg; and prednisolone, 0.2 mg/kg (24, 25). Therapeutic efficacy of bevacizumab was evaluated by survival time. Cyclophosphamide and vincristine were purchased from Shionogi Pharmaceutical Co., Ltd, Osaka, Japan; doxorubicin was from Kyowa Hakko Kirin Co., Ltd, Tokyo, Japan, and prednisolone was from Nippon Kayaku Co., Ltd, Tokyo, Japan.

### Statistical analysis

The differences between groups regarding the tumor necrosis area, vascular number, and human sIL2R concentrations in serum were analyzed by the Mann–Whitney $U$ test. In this study, $P < 0.05$ was considered significant.

## Results

### VEGF-A expression in ATL

VEGF-A expression by ATL cells in the lymph node lesions is shown in Fig. 1A. Immunopathological features of four cases from each group stratified by VEGF-A expression are shown in Fig. 1B. Most of the ATL cases (96%) were positive for VEGF-A.

### ATL cell-bearing NOG mice

In earlier studies, S-YU ATL tumor cells, which were serially transplanted into SCID mice (22), manifested multiple enlarged mesenteric lymph nodes. In the present study, in which NOG mice rather than SCID mice were the S-YU recipients, larger tumor masses formed along the intestinal tract. Figure 2A shows the intraperitoneal masses and intestinal tract adhering tightly to one another in a NOG mouse (demarcated by thin white dotted lines in the figure). Flow cytometric analysis demonstrated that the mass mainly consisted of human cells expressing CD4 and CD25 (Fig. 2B). Immunopathological analysis revealed large atypical cells with irregular and pleomorphic nuclei, and blood vessels. The cells were CD4-positive, CD25-positive, but CD20-negative (Fig. 2C). These findings are consistent with an ATL cell phenotype in humans, and with earlier studies in the SCID/S-YU model. The S-YU tumor cells in the NOG mice were classed as VEGF-A 1+ positive (Fig. 2C). Blood vessels in the tumor tissue were stained by anti-α-SMA Ab (Fig. 2C). Vascular endothelial cells in the tumor tissue were stained by anti-von Willebrand Factor Ab, but not by anti-CD31 mAb (data not shown). Together, these results show that the blood vessels in the tumor tissue originated from the mouse, because anti-α-SMA and von Willebrand Factor Ab used in this study recognized the corresponding protein derived from both human and mouse, whereas the anti-CD31 mAb recognized the corresponding human but not murine protein (data not shown). CD4-positive CD25-positive ATL cell mild infiltration into spleen, liver, and bone marrow was seen by flow cytometry (Fig. 2D).

### VEGF-A, VEGF-R1, and -R2 expression in ATL and HTLV-1-immortalized lines

*VEGF-A mRNA* expression was detected in all 7 ATL and HTLV-1-immortalized lines tested, and in S-YU cells

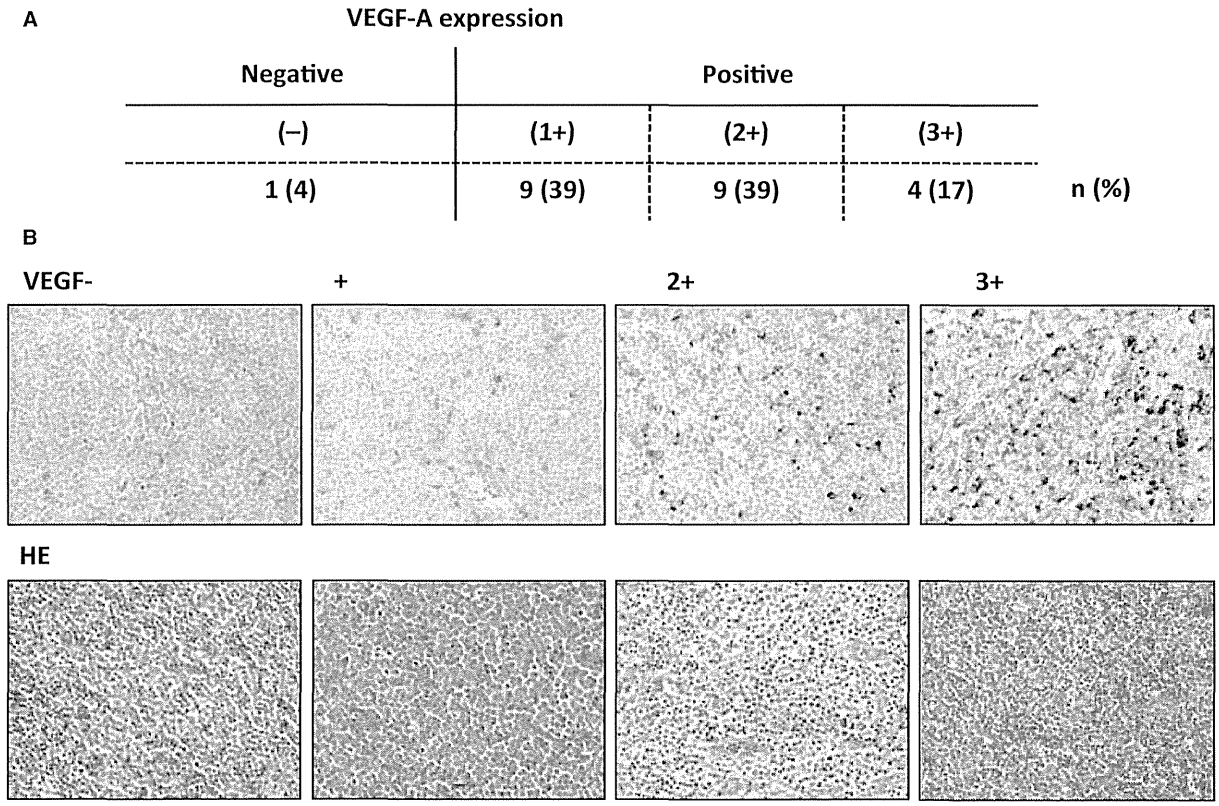


**Figure 1** Vascular endothelial growth factor A (VEGF-A) expression in ATL. (A) VEGF-A expression of ATL cells in the lymph node lesion. VEGF-A expression was categorized based on the percentage of ATL cells stained as follows: ≥50%, 3+ positive; 30–49%, 2+ positive; 10–29%, 1+ positive; <10%, negative. (B) Cases 1, 2, 3, and 4 are representative of VEGF-A-negative, 1+, 2+, and 3+ positive categories, respectively. Photomicrographs with VEGF-A (upper panels) and hematoxylin and eosin staining (lower panels) are shown.

from intraperitoneal masses (Fig. 3A, upper left panel). *VEGF-R1 mRNA* expression was not present in ATL and in only two HTLV-1-immortalized lines (MT-2 and TL-Su) but was present in S-YU cells (Fig. 3A, upper right panel). No *VEGF-R2 mRNA* expression was detected in any of the 7 ATL and HTLV-1-immortalized lines tested, or in S-YU cells (data not shown). Flow cytometry demonstrated that VEGF-R1 protein was also expressed in MT-2 and TL-Su, and very weakly in NOG S-YU cells (Fig. 3A, lower panels), consistent with the RT-PCR results. Flow cytometry demonstrated that VEGF-R2 was not expressed at all in any of the ATL and HTLV-1-immortalized lines tested, or in S-YU cells (data not shown), which was also consistent with the RT-PCR results.

### VEGF-R1 and VEGF-R2 expression in primary ATL cells

CD4-positive CD25-positive primary ATL cells in PBMC obtained from nine individual patients with ATL (i–ix) were evaluated for VEGF-R1 and -R2 expression. VEGF-R1 protein was expressed in only one patient (patient v) and VEGF-R2 was not expressed in any of the patients (Fig. 4B).

### No Bevacizumab-mediated anti-proliferative activity against HTLV-1-immortalized lines and S-YU *in vitro*

Bevacizumab did not directly block the proliferation of MT-2 and TL-Su cells *in vitro*, despite their expression of both VEGF-A and VEGF-R1. Neither did it inhibit S-YU cells (Fig. 3C).

### Therapeutic efficacy of bevacizumab monotherapy in S-YU cell-bearing NOG mice

Photomicrographs of tumor tissue from each mouse are shown (Fig. 4A). Treatment with bevacizumab resulted in an increased percentage of tumor necrosis in the NOG/S-YU mice (mean 25.3%, median 24.1%, range 19.2–33.6%), compared to control mice (mean 15.9%, median 15.4%, range 11.7–21.0%, $P = 0.0060$) (Fig. 4B, left panel). An example of calculating the percentage necrotic area is presented in Fig. 4B, right-hand panels. Bevacizumab treatment resulted in decreased vascular number in the tumor tissues [3.1, 2.6,

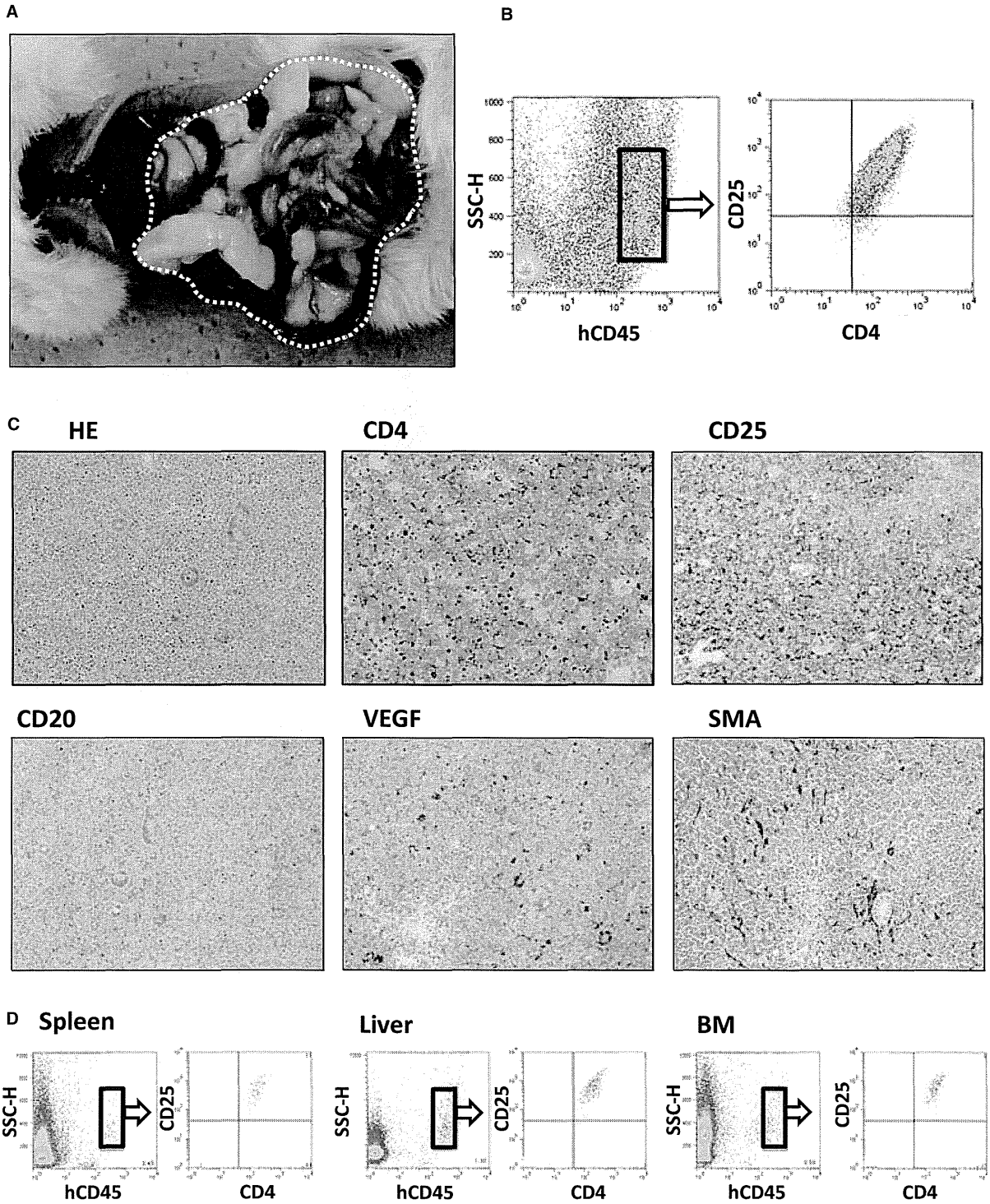


**Figure 2** ATL cell-bearing NOG mouse model. (A) Macroscopic appearance of a primary DLBCL cell-bearing ATL mouse. The intraperitoneal mass is demarcated by a thin white dotted line. (B) Human CD45-positive cells in the mass determined by human CD4 and CD25 expression. (C) Immunohistochemical images of the intraperitoneal mass. (D) Human CD45-positive cells of each organ determined by human CD4 and CD25 expression.

0.0–8.3/mm$^2$; (mean, median, range)], compared to controls (12.8, 15.6, 1.6–19.3/mm$^2$, $P = 0.0127$) (Fig. 4C, left panel). An example of this calculation is presented in Fig. 4C, right-hand panels. Because sIL2R appears in the serum, concomitant with its increased expression on cells, we measured human sIL2R concentrations as a surrogate marker reflecting

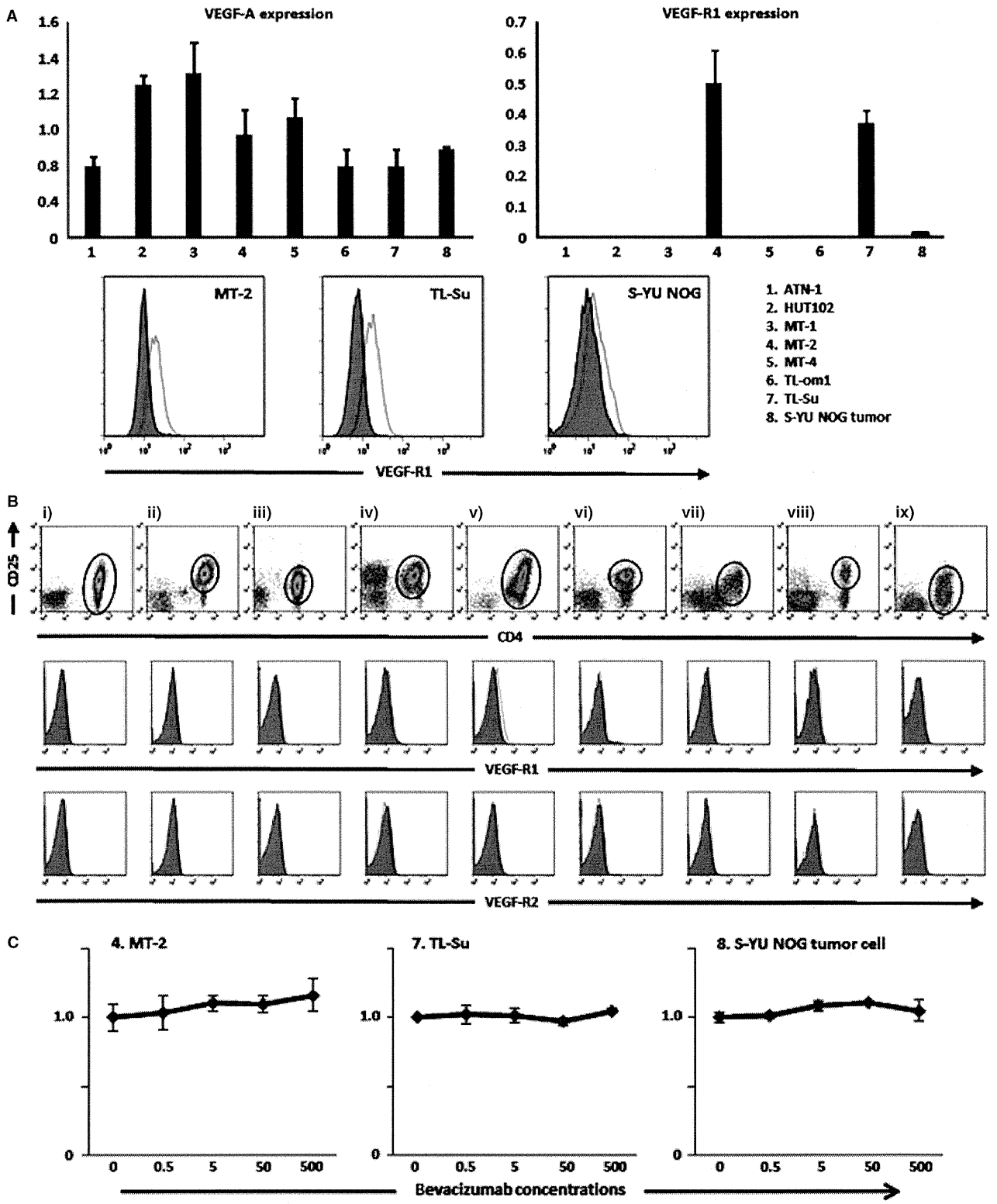


**Figure 3** Vascular endothelial growth factor A (VEGF-A), VEGF-R1, and -R2 expression in primary ATL cells, or ATL and HTLV-1-immortalized lines (A) Quantitative RT-PCR analysis for VEGF-A and VEGF-R1 in 7 ATL and HTLV-1-immortalized lines, and NOG ATL cells from the intraperitoneal mass (upper panels). Flow cytometry for VEGF-R1 in HTLV-1-immortalized lines MT-2 and TL-Su, and NOG ATL cells, from the intraperitoneal mass (lower panels). (B) Flow cytometry for VEGF-R1, and -R2 in 9 primary ATL cells. (C) Bevacizumab has no direct anti-proliferative activity against HTLV-1-immortalized lines (MT-2 and TL-Su) expressing both VEGF-A and VEGF-R1, or NOG ATL cells, *in vitro*. Each result represents three independent experiments.

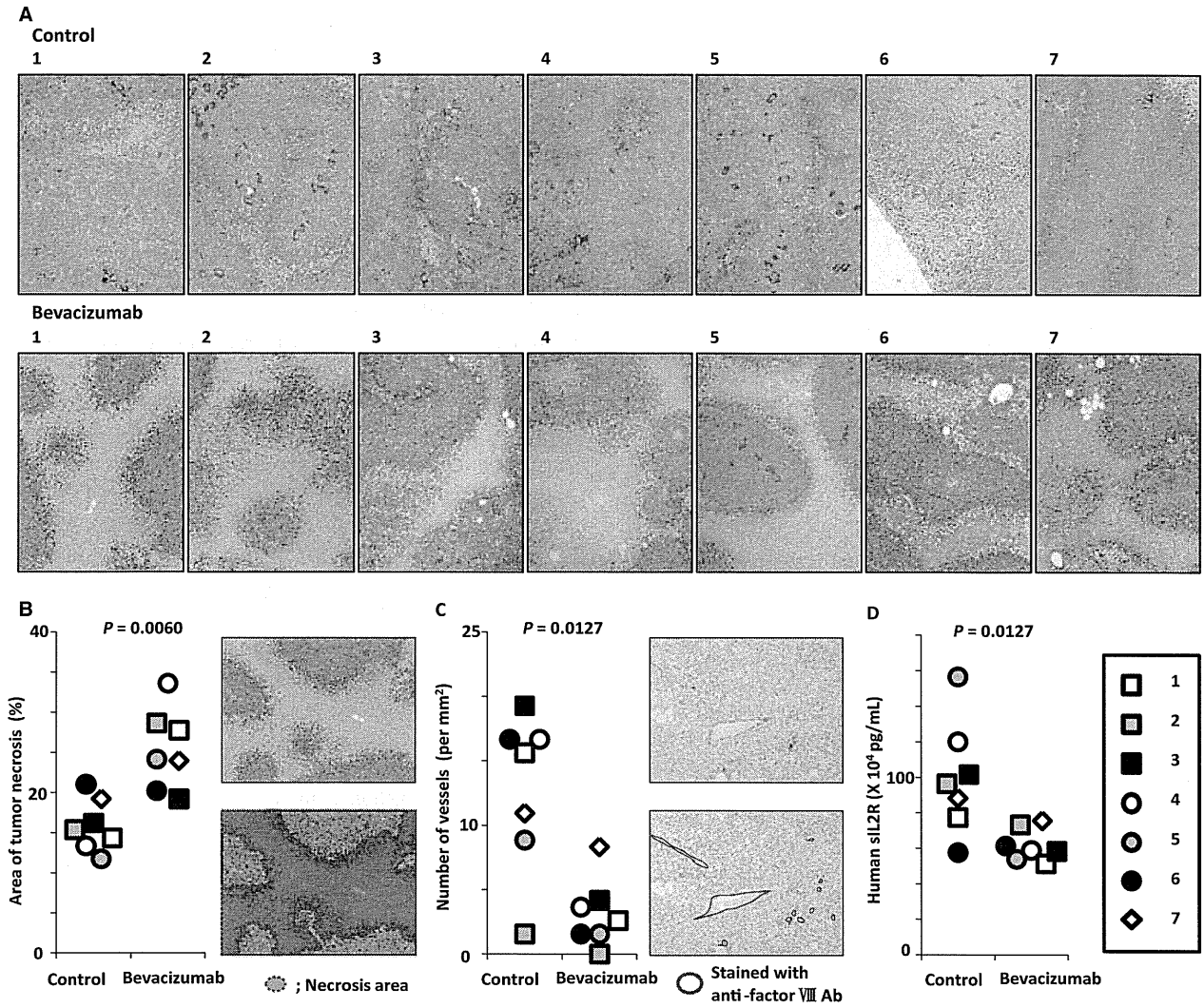


**Figure 4** Bevacizumab therapy has significant therapeutic efficacy in the ATL cell-bearing NOG mouse model. (A) Macroscopic photomicrographs with hematoxylin and eosin staining of mice given saline (control) (upper panels) or bevacizumab (lower panels). (B) Area of tumor necrosis (%) of each ATL cell-bearing NOG mouse. The bevacizumab-treated mice had significantly greater tumor necrosis than control mice (left panel). An example of a calculation for tumor necrosis area (%) by means of Image J software is shown (right panels). (C) Numbers of vessels (/mm$^2$) of each ATL cell-bearing NOG mouse. The bevacizumab recipients had significantly fewer vessels than controls (left panel). An example of such a calculation by means of Image J software is shown (right panels). (D) Serum sIL2R concentrations of each ATL cell-bearing NOG mouse. The bevacizumab recipients had significantly lower levels of sIL2R than controls.

the tumor burden of the human CD25-expressing ATL (26). Treatment with bevacizumab showed significantly greater therapeutic efficacy as demonstrated by sIL2R concentrations in S-YU cell-bearing NOG mice (617.9, 588.5, 513.2–755.7 $\times$ $10^3$ pg/mL), compared to controls (996.6, 963.4, 575.7–1565.0 $\times$ $10^3$ pg/mL, $P$ = 0.0127) (Fig. 4D). Although bevacizumab monotherapy showed significant therapeutic efficacy as demonstrated by the percentage of tumor necrosis, vascular number in the tumor tissues, and sIL2R concentrations in sera (Fig. 4), it did not confer any survival advantage to the NOG/S-YU mice (Fig. 5A). No toxicity attributable to bevacizumab injections was observed in any of the mice in this setting.

### Therapeutic efficacy of bevacizumab plus CHOP compared to CHOP alone in S-YU cell-bearing NOG mice

The bevacizumab plus CHOP group did have a significant prolongation of survival compared with CHOP alone ($P$ = 0.046). The median survival time of bevacizumab plus CHOP and CHOP alone was 38 and 34 d, respectively.

## Discussion

In this study, we have demonstrated that bevacizumab possesses significant therapeutic efficacy in an ATL mouse model in which the tumor cells from a patient survive and

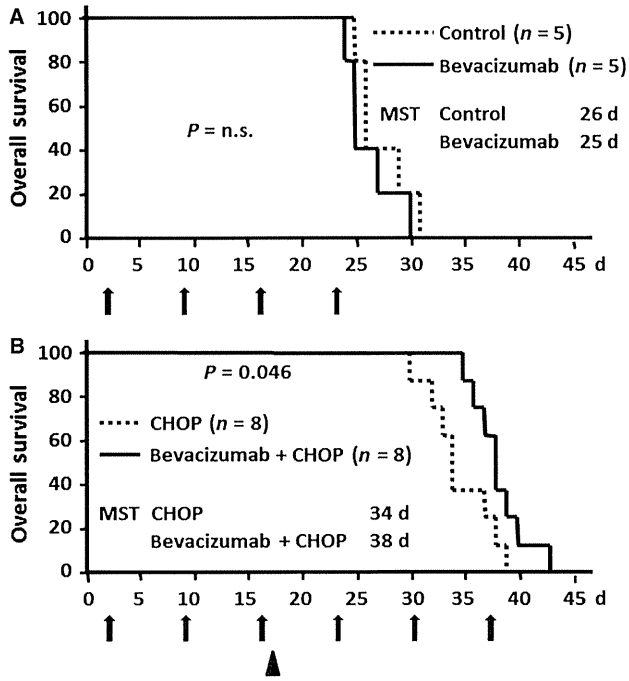


**Figure 5** Survival analysis of ATL cell-bearing NOG mice treated with bevacizumab (A) Kaplan–Meier survival curves of ATL cell-bearing NOG mice treated with bevacizumab or saline. Arrows, bevacizumab or control (saline) injections. Each group consists of five mice. The difference between the bevacizumab and control groups is not significant. (B) Kaplan–Meier survival curves of ATL cell-bearing NOG mice treated with bevacizumab + CHOP, or CHOP alone. Arrows, bevacizumab or control (saline) injections. Arrow head, CHOP injection. Each group consists of eight mice. The difference between the bevacizumab + CHOP and CHOP alone is statistically significant.

proliferate in a murine microenvironment-dependent manner. The present finding revealed the importance of angiogenesis for the pathogenesis of VEGF-expressing ATL.

NOG mice have severe, multiple immune defects, such that human immune cells engrafted into them retain essentially the same functions as in humans (27, 28). While it has been reported that S-YU cells can be serially transplanted into SCID mice as recipients, the present study demonstrated that S-YU cells could also be serially transplanted into NOG mice. This was not unexpected given the even more severe immune dysfunction of NOG mice compared to SCID mice. This may also explain why the ATL tumor masses were much larger in NOG than in SCID mice.

In this study, most primary ATL cases (22/23), and all of the established cell lines tested (7/7), were positive for VEGF-A. These results are consistent with data from other investigators (16, 18, 19). Thus, the VEGF-A produced by ATL cells is likely to play an important role in the pathogenesis of ATL. On the other hand, *VEGF-R1 mRNA* expression was only seen in two of the seven ATL and HTLV-1-immortalized lines, and *VEGF–R2* in none of them. VEGF-R1 protein expression by primary ATL tumor cells was only seen in one of nine patients, and VEGF-R2 in none. In B-cell lymphomas, an earlier study reported that tumor cell growth was promoted in an autocrine fashion via VEGF-A/VEGF-R1 or VEGF-A/VEGF-R2 interactions (29). However, the present analysis of VEGF-R1/R2 expression in ATL, and the results of *in vitro* proliferation assays, did not support the existence of such an autocrine loop in ATL.

Because S-YU cells can only be maintained by serial transplantation in immunodeficient mice, but not by *in vitro* culture (30), the microenvironment is likely to be indispensable for their survival. S-YU are positive for VEGF-A, and therefore it would be expected that the interaction of VEGF-A produced by ATL cells with receptors on host (murine) endothelial cells should play an important role in tumor angiogenesis. This would lead to tumor cell survival and proliferation supported by transport of sufficient nutrients and oxygen in the mouse. Therefore, the present ATL model using S-YU should better reflect the human ATL *in vivo* environment, compared to other mouse models using established ATL cell lines, or HTLV-1-immortalized lines. Thus, this model should provide a powerful tool for understanding the pathogenesis of ATL. Furthermore, it should be useful not only for evaluating novel cytotoxic anti-ATL agents, but also provide a more appropriate *in vivo* model to test antitumor agents targeting the microenvironment, including bevacizumab.

The effect observed in mice receiving bevacizumab monotherapy, as demonstrated by the increased tumor necrosis area and reduced vasculature in the tumor tissue, was expected, given the conventional antitumor mechanism of bevacizumab, which neutralizes the human VEGF-A produced by the tumor cells, but not murine VEGF-A (31). It then inhibits the growth of new blood vessels and thus starves tumor cells of necessary nutrients and oxygen (32). This should lead to a reduced tumor burden, as indicated by the sIL2R concentrations measured. Although bevacizumab monotherapy did show this anti-angiogenesis effect, it did not lead to survival prolongation in this study. This finding is consistent with the clinical observations in many types of cancer such as colorectal cancer, non-small-cell lung cancer, renal cell carcinoma, and ovarian cancer. On the other hand, combination treatment with bevacizumab and CHOP did prolong survival compared to CHOP alone. Nonetheless, the extent of this prolongation was not marked, which is also consistent with clinical observations in many types of cancer where bevacizumab is of limited benefit and then only when combined with chemotherapy. This study suggested that the tumor cell 'starvation effect' alone mediated by bevacizumab does not result in prolonged survival. It has been reported that VEGF-targeted therapy can 'normalize' the tumor vascular network and that this can lead to a more uniform blood flow, with subsequent increased delivery of chemotherapeutic agents (33, 34). This normalization by bevacizumab is a possible explanation for the prolonged survival in the present combination setting.

The present study demonstrated the importance of angiogenesis for the pathogenesis of ATL and the potential efficacy of blocking this in at least a subgroup of patients with ATL. In recent clinical cancer therapy experience, the epidermal growth factor receptor (EGFR) tyrosine kinase inhibitor, gefitinib, failed to yield significantly improved overall survival in patients with refractory NSCLC, but did show therapeutic benefit in a subgroup of patients with mutated EGFR (35). In the case of mAb targeting the EGFR, both panitumumab and cetuximab also yield clinical benefits only in a subgroup of colorectal cancer patients with wild-type *KRAS* and BRAF (36). These findings indicate that we should develop novel treatment strategies based on tumor biology, and not on tumor category. Therefore, as a next step, further investigations are warranted to determine which subgroups of patients with ATL will benefit from bevacizumab therapy (37). In other words, we should face the challenge of developing robust biomarkers that can guide selection of those patients with ATL for whom bevacizumab therapy will be most beneficial. In addition, several promising new agents for treating ATL are currently being developed (1, 38–40). Investigations of combinations of bevacizumab with these novel agents are also warranted.

In conclusion, to the best of our knowledge this is the first report to evaluate the efficacy of bevacizumab for ATL in a tumor microenvironment-dependent animal model. Bevacizumab therapy combined with chemotherapy could be a potential treatment strategy for that subgroup of patients with ATL probably depending to a large extent on angiogenesis via VEGF for tumor survival and proliferation.

## Acknowledgements

We thank Ms Chiori Fukuyama for her excellent technical assistance and Ms. Naomi Ochiai for her excellent secretarial assistance.

## Funding

This study was supported by Grants-in-Aid for Scientific Research (B) (No. 25290058, T. Ishida), and Scientific Support Programs for Cancer Research (No. 221S0001, T. Ishida) from the Ministry of Education, Culture, Sports, Science and Technology of Japan, Grants-in-Aid for National Cancer Center Research and Development Fund (No. 21-6-3, T. Ishida), and H23-Third Term Comprehensive Control Research for Cancer-general-011, T. Ishida, from the Ministry of Health, Labour and Welfare, Japan.

## Authorship contributions

Mori F, Ishida T, Asahi I, and Ueda R designed the research. Mori F, Ishida T, Asahi I, Sato F, Masaki A, Narita T, Suzuki S, Yamada T, and Takino H performed the research. Hishizawa M, Imada K, Takaori-Kondo A contributed to establishing the ATL mouse model. All the authors analyzed the data and wrote the article.

## Conflict of interest

Nagoya City University Graduate School of Medical Sciences has received research funding for Takashi Ishida, Shigeru Kusumoto, and Shinsuke Iida from Chugai Pharmaceutical Co., Ltd. The other authors have no financial conflicts of interest related with this study.

## References

1. Ishida T, Ueda R. Antibody therapy for adult T-cell leukemia-lymphoma. *Int J Hematol* 2011;**94**:443–52.
2. Matsuoka M, Jeang KT. Human T-cell leukaemia virus type 1 (HTLV-1) infectivity and cellular transformation. *Nat Rev Cancer* 2007;**7**:270–80.
3. Shimoyama M. Diagnostic criteria and classification of clinical subtypes of adult T-cell leukaemia-lymphoma. A report from the Lymphoma Study Group (1984–87). *Br J Haematol* 1991;**79**:428–37.
4. Uchiyama T, Yodoi J, Sagawa K, Takatsuki K, Uchino H. Adult T-cell leukemia: clinical and hematologic features of 16 cases. *Blood* 1977;**50**:481–92.
5. Ishida T, Hishizawa M, Kato K, *et al.* Allogeneic hematopoietic stem cell transplantation for adult T-cell leukemia-lymphoma with special emphasis on preconditioning regimen: a nationwide retrospective study. *Blood* 2012;**120**:1734–41.
6. Utsunomiya A, Miyazaki Y, Takatsuka Y, *et al.* Improved outcome of adult T cell leukemia/lymphoma with allogeneic hematopoietic stem cell transplantation. *Bone Marrow Transplant* 2001;**27**:15–20.
7. Carmeliet P, Jain RK. Molecular mechanisms and clinical applications of angiogenesis. *Nature* 2011;**473**:298–307.
8. Burger RA, Brady MF, Bookman MA, *et al.* Incorporation of bevacizumab in the primary treatment of ovarian cancer. *N Engl J Med* 2011;**365**:2473–83.
9. Escudier B, Pluzanska A, Koralewski P, *et al.* Bevacizumab plus interferon alfa-2a for treatment of metastatic renal cell carcinoma: a randomised, double-blind phase III trial. *Lancet* 2007;**370**:2103–11.
10. Escudier B, Bellmunt J, Négrier S, Bajetta E, Melichar B, Bracarda S, Ravaud A, Golding S, Jethwa S, Sneller V. Phase III trial of bevacizumab plus interferon alfa-2a in patients with metastatic renal cell carcinoma (AVOREN): final analysis of overall survival. *J Clin Oncol* 2010;**28**:2144–50.
11. Hurwitz H, Fehrenbacher L, Novotny W, *et al.* Bevacizumab plus irinotecan, fluorouracil, and leucovorin for metastatic colorectal cancer. *N Engl J Med* 2004;**350**:2335–42.
12. Perren TJ, Swart AM, Pfisterer J, *et al.* A phase 3 trial of bevacizumab in ovarian cancer. *N Engl J Med* 2011;**365**:2484–96.

13. Sandler A, Gray R, Perry MC, Brahmer J, Schiller JH, Dowlati A, Lilenbaum R, Johnson DH. Paclitaxel-carboplatin alone or with bevacizumab for non-small-cell lung cancer. *N Engl J Med* 2006;**355**:2542–50.
14. Yang JC, Haworth L, Sherry RM, Hwu P, Schwartzentruber DJ, Topalian SL, Steinberg SM, Chen HX, Rosenberg SA. A randomized trial of bevacizumab, an anti-vascular endothelial growth factor antibody, for metastatic renal cancer. *N Engl J Med* 2003;**349**:427–34.
15. Kreisl TN, Kim L, Moore K, *et al.* Phase II trial of single-agent bevacizumab followed by bevacizumab plus irinotecan at tumor progression in recurrent glioblastoma. *J Clin Oncol* 2009;**27**:740–5.
16. Bazarbachi A, Abou Merhi R, Gessain A, *et al.* Human T-cell lymphotropic virus type I-infected cells extravasate through the endothelial barrier by a local angiogenesis-like mechanism. *Cancer Res* 2004;**64**:2039–46.
17. El-Sabban ME, Merhi RA, Haidar HA, Arnulf B, Khoury H, Basbous J, Nijmeh J, de Thé H, Hermine O, Bazarbachi A. Human T-cell lymphotropic virus type 1-transformed cells induce angiogenesis and establish functional gap junctions with endothelial cells. *Blood* 2002;**99**:3383–9.
18. Hayashibara T, Yamada Y, Miyanishi T, Mori H, Joh T, Maeda T, Mori N, Maita T, Kamihira S, Tomonaga M. Vascular endothelial growth factor and cellular chemotaxis: a possible autocrine pathway in adult T-cell leukemia cell invasion. *Clin Cancer Res* 2001;**7**:2719–26.
19. Watters KM, Dean J, Gautier V, Hall WW, Sheehy N. Tax 1-independent induction of vascular endothelial growth factor in adult T-cell leukemia caused by human T-cell leukemia virus type 1. *J Virol* 2010;**84**:5222–8.
20. Ito M, Kobayashi K, Nakahata T. NOD/Shi-scid IL2rgnull (NOG) mice more appropriate for humanized mouse models. *Curr Top Microbiol Immunol* 2008;**324**:53–76.
21. Abramoff MD, Magelhaes PJ, Ram SJ. Image Processing with ImageJ. *Biophotonics Int* 2004;**11**:36–42.
22. Imada K, Takaori-Kondo A, Sawada H, Imura A, Kawamata S, Okuma M, Uchiyama T. Serial transplantation of adult T cell leukemia cells into severe combined immunodeficient mice. *Jpn J Cancer Res* 1996;**87**:887–92.
23. Suzuki S, Masaki A, Ishida T, *et al.* Tax is a potential molecular target for immunotherapy of adult T-cell leukemia/lymphoma. *Cancer Sci* 2012;**103**:1764–73.
24. Mori F, Ishida T, Ito A, *et al.* Potent antitumor effects of bevacizumab in a microenvironment-dependent human lymphoma mouse model. *Blood Cancer J* 2012;**2**:e67.
25. Mohammad RM, Wall NR, Dutcher JA, Al-Katib AM. The addition of bryostatin 1 to cyclophosphamide, doxorubicin, vincristine, and prednisone (CHOP) chemotherapy improves response in a CHOP-resistant human diffuse large cell lymphoma xenograft model. *Clin Cancer Res* 2000;**6**:4950–6.
26. Motoi T, Uchiyama T, Uchino H, Ueda R, Araki K. Serum soluble interleukin-2 receptor levels in patients with adult T-cell leukemia and human T-cell leukemia/lymphoma virus type-I seropositive healthy carriers. *Jpn J Cancer Res* 1988;**79**:593–9.
27. Ito A, Ishida T, Utsunomiya A, *et al.* Defucosylated anti-CCR4 monoclonal antibody exerts potent ADCC against primary ATLL cells mediated by autologous human immune cells in NOD/Shi-scid, IL-2R gamma(null) mice *in vivo*. *J Immunol* 2009;**183**:4782–91.
28. Masaki A, Ishida T, Suzuki S, *et al.* Autologous Tax-Specific CTL therapy in a primary adult T cell leukemia/lymphoma cell-bearing NOD/Shi-scid, IL-2Rγnull mouse model. *J Immunol* 2013;**191**:135–44.
29. Wang ES, Teruya-Feldstein J, Wu Y, Zhu Z, Hicklin DJ, Moore MA. Targeting autocrine and paracrine VEGF receptor pathways inhibits human lymphoma xenografts *in vivo*. *Blood* 2004;**104**:2893–902.
30. Koga H, Imada K, Ueda M, Hishizawa M, Uchiyama T. Identification of differentially expressed molecules in adult T-cell leukemia cells proliferating *in vivo*. *Cancer Sci* 2004;**95**:411–7.
31. Yu L, Wu X, Cheng Z, Lee CV, LeCouter J, Campa C, Fuh G, Lowman H, Ferrara N. Interaction between bevacizumab and murine VEGF-A: a reassessment. *Invest Ophthalmol Vis Sci* 2008;**49**:522–7.
32. Ellis LM, Hicklin DJ. VEGF-targeted therapy: mechanisms of anti-tumour activity. *Nat Rev Cancer* 2008;**8**:579–91.
33. Carmeliet P, Jain RK. Principles and mechanisms of vessel normalization for cancer and other angiogenic diseases. *Nat Rev Drug Discov* 2011;**10**:417–27.
34. Jain RK. Normalization of tumor vasculature: an emerging concept in antiangiogenic therapy. *Science* 2005;**307**:58–62.
35. Maemondo M, Inoue A, Kobayashi K, *et al.* Gefitinib or chemotherapy for non-small-cell lung cancer with mutated EGFR. *N Engl J Med* 2010;**362**:2380–8.
36. Bardelli A, Siena S. Molecular mechanisms of resistance to cetuximab and panitumumab in colorectal cancer. *J Clin Oncol* 2010;**28**:1254–61.
37. Lambrechts D, Lenz HJ, de Haas S, Carmeliet P, Scherer SJ. Markers of response for the antiangiogenic agent bevacizumab. *J Clin Oncol* 2013;**31**:1219–30.
38. Ishida T, Joh T, Uike N, *et al.* Defucosylated anti-CCR4 monoclonal antibody (KW-0761) for relapsed adult T-cell leukemia-lymphoma: a multicenter phase II study. *J Clin Oncol* 2012;**30**:837–42.
39. Tanosaki R, Tobinai K. Adult T-cell leukemia-lymphoma: current treatment strategies and novel immunological approaches. *Expert Rev Hematol* 2010;**3**:743–53.
40. Marçais A, Suarez F, Sibon D, Frenzel L, Hermine O, Bazarbachi A. Therapeutic options for adult T-cell leukemia/lymphoma. *Curr Oncol Rep* 2013;**15**:457–64.

Human Pathology (2014) 45, 1192–1198

ELSEVIER

Human PATHOLOGY

www.elsevier.com/locate/humpath

Original contribution

# Prognostic impact of microRNA-145 down-regulation in adult T-cell leukemia/lymphoma☆,☆☆

Hongjing Xia MD, PhD[a,1], Seiji Yamada MD, PhD[a,1], Mineyoshi Aoyama MD, PhD[b,1], Fumihiko Sato DMD, PhD[a], Ayako Masaki MD, PhD[a], Yan Ge MD[a], Masaki Ri MD, PhD[c], Takashi Ishida MD, PhD[c], Ryuzo Ueda MD, PhD[c,d], Atae Utsunomiya MD, PhD[e], Kiyofumi Asai MD, PhD[b], Hiroshi Inagaki MD, PhD[a,*]

[a]*Department of Anatomic Pathology and Molecular Diagnostics, Nagoya City University Graduate School of Medical Sciences, Nagoya 467-8601, Japan*
[b]*Department of Molecular Neurobiology, Nagoya City University Graduate School of Medical Sciences, Nagoya 467-8601, Japan*
[c]*Department of Medical Oncology and Immunology, Nagoya City University Graduate School of Medical Sciences, Nagoya 467-8601, Japan*
[d]*Department of Tumor Immunology, Aichi Medical University School of Medicine, Nagakute 480-1195, Japan*
[e]*Department of Hematology, Imamura Bun-in Hospital, Kagoshima 890-0064, Japan*

Received 17 October 2013; revised 16 January 2014; accepted 24 January 2014

**Keywords:**
Adult T-cell leukemia/lymphoma;
Prognosis;
MicroRNAs;
Array analysis;
miR-145

**Summary** Adult T-cell leukemia/lymphoma (ATL) is a highly aggressive tumor caused by human T-cell leukemia virus type 1. MicroRNAs (miRNAs) are closely involved in the development and progression of various tumors. Here we investigated the dysregulation of miRNAs in ATL and its clinical significance. Studies using miRNA arrays and subsequent real-time reverse transcription polymerase chain reaction showed that, in the 9 ATL cell lines examined, 1 miRNA was consistently up-regulated, whereas another 3 were consistently down-regulated, compared with normal CD4-positive lymphocytes. Next, we analyzed the prognostic impact of these 4 miRNAs in patients with aggressive-type ATL (n = 40). Of the 4 dysregulated miRNAs selected, 3 (miR-130b higher expression, miR-145 lower expression, and miR-223 lower expression) were significantly associated with a worsened overall patient survival. We found that expressions of these 3 miRNAs were correlated with each other. To clarify which of the 3 had the most significant impact on overall survival, we performed a multivariate prognostic analysis that included these 3 miRNAs, and only miR-145 lower expression was selected as an independent risk factor ($P = .0005$). When overexpressed in an ATL cell line in vitro, miR-145 specifically inhibited tumor cell growth. In conclusion, our study suggests that miR-145 down-regulation provides a growth advantage in ATL and is highly associated with a worsened prognosis for patients with ALT. Hence, miR-145 may be a useful prognostic marker and a potential therapeutic target for ATL.


☆ Funding/Support: This study was supported in part by a Grant-in-Aid for Scientific Research from the Ministry of Education, Culture, Sports, Science, and Technology (MEXT), Japan, and by a Grant-in-Aid from the Ministry of Health, Labor, and Welfare.
☆☆ Competing interests: None.
* Corresponding author.
*E-mail address:* hinagaki@med.nagoya-cu.ac.jp (H. Inagaki).
[1] These authors contributed equally to this work.

http://dx.doi.org/10.1016/j.humpath.2014.01.017
0046-8177/

## 1. Introduction

MicroRNAs (miRNAs) are 18- to 25-nucleotide, single-stranded noncoding RNA molecules that play an important regulatory role by targeting mRNAs for repressing translation or mRNA cleavage [1]. They are transcribed with primary miRNAs, transported into the cytoplasm, cleaved into mature miRNAs, and then loaded onto the miRNA-induced silencing complex for RNA interference. The miRNA-induced silencing complex is guided to its mRNA target by the miRNA strand, which typically base pairs imperfectly to its target in the 3′ untranslated region, signaling the target for translational repression or degradation. Global changes of miRNAs are closely involved in neoplastic processes and tumor progression, and differential expression of miRNAs has been described in various tumors [2,3].

Human T-cell leukemia virus type 1 (HTLV-1) is a retrovirus known to be an etiologic agent of adult T-cell leukemia/lymphoma (ATL) [4]. More than 20 million people are infected with HTLV-1 worldwide, with the highest prevalence in southwest Japan and the Caribbean basin. HTLV-1 infection has a long clinical latency before transforming into ATL. It has a very poor prognosis because tumor cells are usually resistant to conventional chemotherapeutic agents [5,6]. Patients with ATL are typically highly immunocompromised and have frequent severe infections. Tumor cells from most patients with ATL are positive for CD4, CD25, and FOXP3. These immunologic and phenotypic characteristics of ATL are similar to those of regulatory T cells, and it has been suggested that ATL cells may originate from regulatory T cells, which actively suppress activation of the immune system [7].

Recently, some miRNAs have been shown to be involved in ATL [8-13]. However, oncogenetic and clinical significance of miRNAs have not been well clarified. In this study, we examined ATL cell lines and clinical ATL cases for miRNA expression using miRNA arrays, quantitative reverse transcription (RT) polymerase chain reaction (PCR), and the miRNA transfection assay.

## 2. Materials and methods

### 2.1. ATL cell lines and normal CD4-positive T cells

The 9 cell lines used in this study were as follows; ATL-102, ATN-1, HUT-102, MJ, MT-1, MT-2, MT-4, TL-Om1, and TL-SU. These cell lines were cultured in RPMI 1640 media supplemented with 10% fetal bovine serum, 50 U/mL penicillin, and 50 μg/mL streptomycin (Invitrogen, GIBCO, Carlsbad, CA), at 37°C with 5% $CO_2$. Mononuclear cells obtained from healthy volunteers (n = 4) were sorted into CD4-positive T cells.

### 2.2. Patients with ATL

Forty specimens from patients with aggressive ATL of the acute- or lymphoma-type [5] were retrieved from the pathology files of Nagoya City University, Graduate School of Medical Sciences, and Imamura Bun-in Hospital. All specimens were obtained at the initial presentation of the patients and were fixed in formalin and embedded in paraffin. All cases were positive for monoclonal integration of HTLV-1 provirus DNA. The pathological specimens were reviewed according to criteria of the World Health Organization classification of malignant lymphomas [6]. The median age at diagnosis was 60 years (range, 42-88 years), with a male-to-female ratio of approximately 1:1. All cases were within the morphologic boundaries of ATL and exhibited the following immunophenotypes: CD20−, CD3+, CD5+, CD4+, and CD25+. Thirty-three cases were histologically classified as the pleomorphic medium-large cell type, 3 as the pleomorphic small cell type, 3 as the anaplastic type, and 1 as the Hodgkin-like type. All patients were treated with doxorubicin-containing combination chemotherapy regimens. The study was approved by the institutional review board of Nagoya City University.

### 2.3. miRNA expression array

Using a flash PAGE system (Ambion, Carlsbad, CA), miRNA was extracted from 4 ATL cell lines (ATN-1, HUT-102, MJ, and TL-Om1). For the miRNA microarray, CD4-positive T-cell samples obtained from peripheral blood of 4 healthy volunteers were evenly mixed, and miRNA was extracted and used as a control miRNA. ATL has been suggested to originate from regulatory T cells, which are less than 2% of total CD4-positive cells in peripheral blood [14] and include 2 subsets, naturally occurring and inducible types [15]. Because it was difficult to obtain sufficient numbers of regulatory T cells for the experiment and to induce regulatory T cells specifically, we used CD4-positive T cells as a control in this study. miRNA samples were labeled with Cy-5 using a Label IT miRNA Labeling kit (Mirus Bio, Madison, WI) and hybridized to the array slides (mirVana miRNA Bioarray V2; Ambion). Signals were scanned with an Axon GenePix 4000B scanner (Molecular Devices, Sunnyvale, CA), and the miRNA array data thus obtained were analyzed using a Microarray Data Analysis Tool (Filgen, Nagoya, Japan) to select miRNAs significantly up- or down-regulated in all 4 ATL lines compared with control normal CD4-positive T cells.

### 2.4. miRNA isolation and quantitative RT-PCR in ATL cell lines

Total RNA extracted from fresh ATL cell lines (n = 9) and normal CD4-positive T cells from the 4 healthy volunteers was further miRNA-enriched using a PureLink miRNA

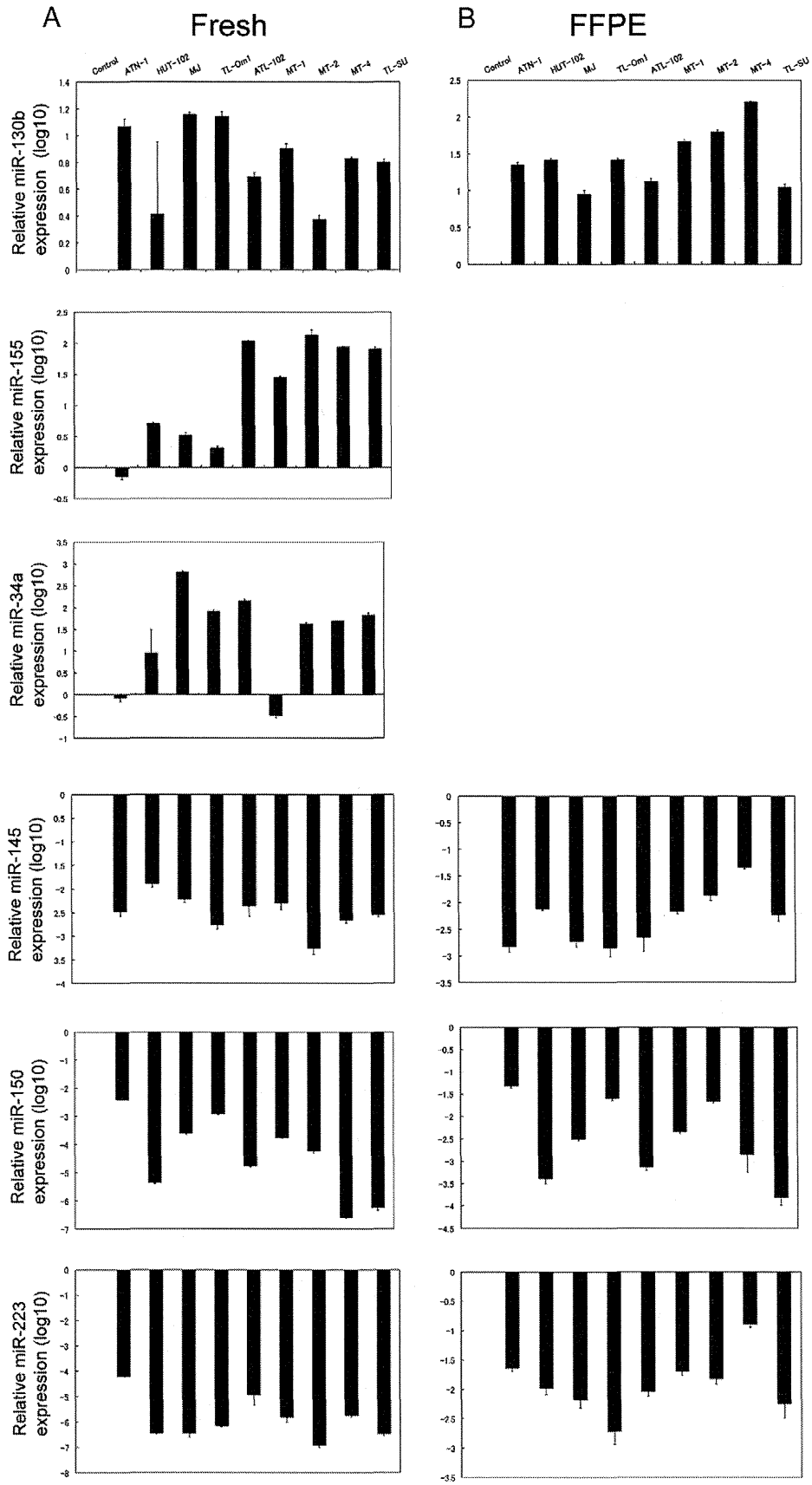


**Fig. 1** Relative expression (log 10) of 6 miRNAs (miR-130b, miR-155, miR-34a, miR-145, miR-150, and miR-223) in 9 ATL cell lines (ATN-1, HUT102, MJ, TL-Om1, ATL-102, MT-1, MT-2, MT-4, and TL-SU). The 6 graphs (A) show levels using fresh ATL cell lines, and the 4 graphs (B) show levels using formalin-fixed, paraffin-embedded (FFPE) ATL cell lines.

Isolation kit (Invitrogen, Tokyo, Japan). Quantitative RT-PCR for the targeted mature miRNAs was performed using TaqMan MicroRNA Reverse Transcription kit (Applied Biosystems, Foster City, CA) and a TaqMan MicroRNA Assay kit (Applied Biosystems). All PCR reactions were run in triplicate, and miRNA expression relative to control RNU6B was calculated using the $2^{-\Delta\Delta Ct}$ method. The expression of miRNAs in T cells from the 4 healthy individuals was used as a quantitative control. ATL cell lines were fixed in formalin and embedded in paraffin. miRNAs extracted from the paraffin sections were subjected to quantitative RT-PCR to confirm that the target miRNAs were correctly quantified using paraffin sections as well.

### 2.5. miRNA expression in patients with ATL

Enriched total miRNA was extracted from paraffin-embedded materials of CD4-positive T cells from healthy patients and patients with ATL. Expression of target miRNAs was similarly semiquantified using quantitative RT-PCR. Cutoff values for higher or lower expression of respective miRNAs were set to give superior segregation into prognostic groups in overall survival. For patients with ATL, selected miRNAs were correlated with various clinicopathological factors (age, sex, the presence of B symptoms, extranodal sites, bone marrow involvement, serum lactate dehydrogenase (LDH) values more than twice the normal upper limit [5], histologic lymphoma subtype, and overall survival of the patients).

### 2.6. miRNA transfection and cell viability and death

MT-4 ATL cells ($2 \times 10^6$) were resuspended in 100 $\mu$L of Nucleofector solution (Cell Line Nucleofector Kit V; Amaxa Biosystems, Cologne, Germany). Cells were electroporated with 100 and 300 nmol/L pre-miR has-miR-145 miRNA precursor, and a pre-miR negative control no. 1 using a Nucleofector (Pre-miR miRNA precursor Starter Kit; Ambion). Transfected cells were plated onto 6-well plates, and 1 mL/well antibiotic-free medium was added for incubation at 37°C with 5% $CO_2$. After 6 hours, 1.5 mL/well RPMI 1640 media supplemented with 10% fetal bovine serum, 50 U/mL penicillin, and 50 $\mu$g/mL streptomycin were added. Cells were plated in 96-well plates at $6 \times 10^3$ cells/well and cultured for 0, 24, 48, and 72 hours to test their viability using a methyl thiazolyl tetrazorium (MTT). The remaining cells were extracted for miRNA using an miRNA Isolation kit (Invitrogen) to verify electroporation quality.

### 2.7. Statistical analysis

All statistical analyses were performed using JMP (SAS, Cary, NC). The relationship between miRNA expression and various clinicopathological factors was evaluated using the Mann-Whitney *U* test or Fisher exact test. Survival curves were plotted using the Kaplan-Meier method, and the Cox proportional hazards model was applied for univariate and multivariate prognostic analysis. The in vitro data were analyzed using a paired *t* test. A probability value of $P < .05$ was regarded as statistically significant. All tests were 2 tailed.

## 3. Results

### 3.1. miRNA array analysis using ATL cell lines

Using miRNA array analysis, we profiled 4 ATL cell lines (ATN-1, HUT-102, MJ, and TL-Om1) using normal CD4-positive T cells as a control. In these 4 ATL cell lines, 3 miRNAs (miR-34a, miR-130b, and miR-155) were consistently highly up-regulated, and 3 miRNAs (miR-145, miR-150, and miR-223) were consistently highly down-regulated (Supplementary Fig. S1). To confirm the results of miRNA array data, we quantified these 6 miRNAs using quantitative real-time RT-PCR with the fresh 9 ATL cell lines (ATN-1, HUT-102, MJ, TL-Om1, ATL-102, MT-1, MT-2, MT-4, and TL-SU), including the 4 ATL cell lines used for miRNA array analysis (Fig. 1A). Of the 6 miRNAs tested, 4 (miR-130b, miR-145, miR-223, and miR-150) were consistently up- or down-regulated in the 9 ATL cell lines (Fig. 1A). Although up-regulated in the miRNA array, miR-34a and miR-155 were down-regulated in 1 and 2 of the 9 ATL cell lines, respectively (Fig. 1A), and we excluded these 2 miRNAs. The remaining 4 miRNAs were precisely quantified by quantitative RT-PCR using formalin-fixed, paraffin-embedded ATL cell lines as well (Fig. 1B).

**Table** Univariate and multivariate prognostic analyses of miRNAs for overall survival of the patients with ATL

| miRNA | Expression | Overall survival | | | | | |
|---|---|---|---|---|---|---|---|
| | | Univariate | | | Multivariate | | |
| | | *P* | Hazard ratio | 95% CI | *P* | Hazard ratio | 95% CI |
| miR130b | Higher | .0017 | 1.83 | 1.24-2.83 | NS | | |
| miR145 | Lower | <.0001 | 3.01 | 1.79-5.16 | .0005 | 2.59 | 1.52-4.49 |
| miR150 | Lower | NS | | | | | |
| miR223 | Lower | .0010 | 0.96 | 1.29-3.25 | NS | | |

Abbreviations: CI, confidence interval; NS, not significant.

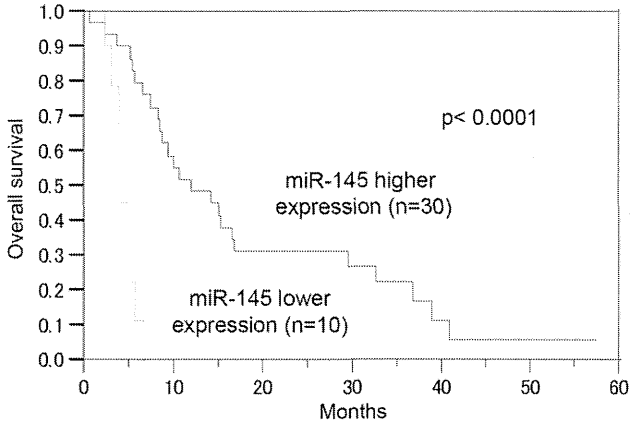


**Fig. 2** Overall survival analysis of patients with ATL for miR-145 expression.

### 3.2. Expression of miRNAs in clinical ATL samples

Using quantitative RT-PCR, 40 clinical ATL cases (paraffin-embedded tumor samples) were examined for expression levels of the selected 4 miRNAs (miR-130b, miR-145, miR-150, and miR-223). To explore miRNAs highly associated with the clinical course, the prognostic impact of the 4 miRNAs on the overall survival of patients with ATL was analyzed. As shown in the Table, using a respective cutoff value that showed superior segregation into prognostic groups, 28 cases were higher expressers for miR-130b ($P = .0017$) and 10 cases each were lower expressers for miR-145 ($P < .0001$) and miR-223 ($P = .0010$). Expression of miR-150 failed to show any prognostic impact. The 3 miRNAs that showed a prognostic impact

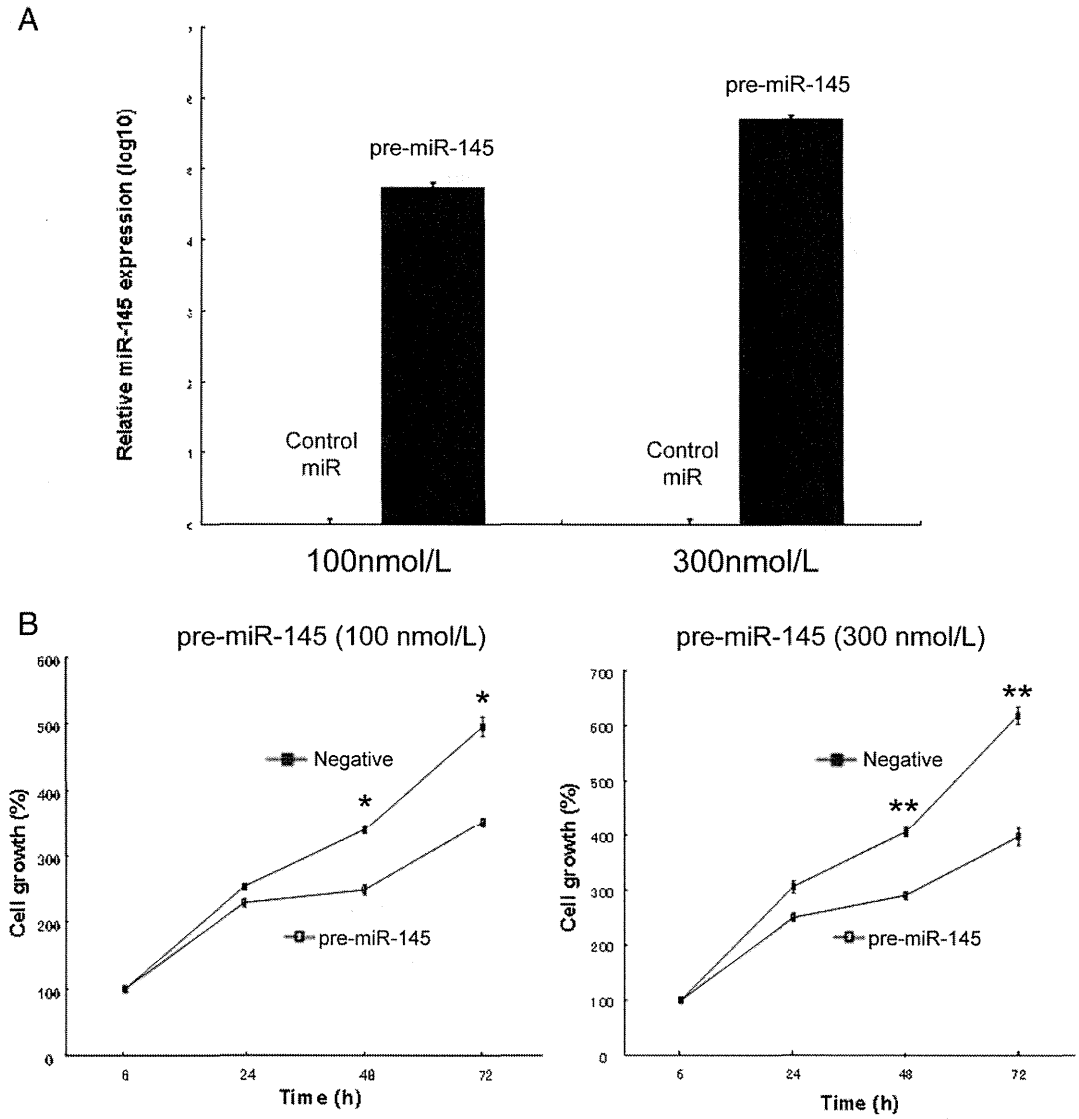


**Fig. 3** miR-145 transfection assay. A, Relative expression (log 10) of miR-145 in ATL cells (MT-4) transfected with pre–miR-145 precursor or with negative control pre-miRNA precursor after a 48-hour incubation at a final concentration of 100 (left) or 300 nM (right). B, The effect of pre–miR-145 on growth of ATL cells (MT-4) as determined by an MTT assay. Cell proliferation is significantly inhibited by enforced expression of miR-145. The data represent the means ± SEM of 4 independent experiments. $*P < .05$ and $**P < .01$.

were found to be associated with each other (miR-130b versus miR-145, $P = .019$; miR-130b versus miR-223, $P < .0001$; and miR-145 versus miR-223, $P = .043$). To explore which miRNA was the most associated with the patients' prognosis, we performed a multivariate analysis. Only miR-145 lower expression was selected as a prognostic factor ($P = .0005$; hazard ratio, 2.59 [1.52-4.49]), whereas the other 2 miRNAs failed to achieve statistical significance (Table). Fig. 2 shows the overall survival curve of patients with ATL for miR-145 expression. miR-145 expression of patients with ATL relative to that of normal CD4-positive T cells was 0.0495 ± 0.0276 and 3.02 ± 1.03 (mean ± SEM) for lower and higher expressers, respectively. When correlated with clinicopathological factors including age, sex, the presence of B symptoms, performance status, extranodal sites, bone marrow involvement, elevated LDH value, and histologic lymphoma subtype, miR-145 lower expression was not associated with any of these factors.

### 3.3. Overexpression of miR-145 and cell growth inhibition in ATL cells

Because miR-145 was consistently down-regulated in ATL cell lines and showed the highest prognostic impact on patients' survival, we focused on this miRNA in further analysis. To examine the association between miR-145 expression and the growth of ATL cells, MT-4 cells were transfected with a pre–miR-145 precursor and a pre-miR negative control, and an MTT assay was conducted. Overexpression of mature miR-145 in the transfected cells was confirmed by quantitative RT-PCR (Fig. 3A). Cell growth was significantly inhibited in cells transfected with pre–miR-145 48 hours after the transfection by approximately 40% as compared with those transfected with the pre-miR negative control (Fig. 3B). These results indicated that miR-145 specifically inhibited the cell growth of the MT-4 cell line.

## 4. Discussion

In this study, we found that 1 miRNA (miR-130b) was consistently up-regulated, and 3 (miR-145, miR-223, and miR-150) were consistently down-regulated in ATL cell lines using an miRNA array and subsequent quantitative RT-PCR. It has been shown that expression of some of these miRNAs is dysregulated in ATL cell lines: miR-130b and miR223 have been reported to be up-regulated [8] and down-regulated [10], respectively. miR155, which was selected in the present miRNA array but was subsequently excluded because of its inconsistent expression in the quantitative RT-PCR, has been frequently up-regulated in ATL [9,10,13]. It is difficult to explain this discrepancy. A similar observation was reported in cutaneous T-cell lymphoma, and it was speculated that cross-hybridization of pre–miR-155 to the hybridization probe might have masked the signal of the mature miR-155 [16]. Recently, Yamagishi et al [11] and Tomita et al [12] determined the miRNA signatures and revealed miR-31 down-regulation and miR-146a up-regulation in primary ATL cells, respectively. However, these 2 miRNAs were not highly dysregulated in our miRNA array. This is partly explained by our use of the ATL tumor samples and control samples. For the ATL tumor samples and controls, we used ATL cell lines and normal CD4-positive lymphocytes while Yamagishi et al used clinical ATL cells as tumor samples [11] and Tomita et al used HTLV-1–uninfected T-cell lines as a control [12].

Of the 4 dysregulated miRNAs we determined (miR-130b, miR-145, miR-150, and miR-223), we searched for miRNAs that had a prognostic impact on clinical ATL cases. For each of the 4 miRNAs, we divided our ATL cases into 2 groups (higher and lower expression) using a respective cutoff value that showed superior segregation into prognostic groups. Univariate prognostic analysis showed that miR-130b, miR-145, and miR-223, but not miR-150, had a significant association with the overall survival of patients with ATL. The reason why miR-150 did not achieve statistical significance is difficult to discern, but may be partly explained as follows. First, some miRNAs are expressed differently in ATL cell lines compared with clinical samples, and miR-150 was reported to be differentially expressed in ATL cell lines and uncultured ATL cells [9]. Second, miR-150 may be more associated with tumor development than tumor progression.

We found that the expressions of 3 selected miRNAs (miR-130b, miR-145, and miR-223) were significantly associated with each other. Multivariate prognostic analysis including these 3 miRNAs revealed that only miR-145 lower expression achieved statistical significance. Interestingly, this miRNA was not correlated with any of the clinicopathological or risk factors examined, suggesting that miR-145 lower expression might be a useful independent prognostic factor. Although down-regulated in all ATL cell lines examined, miR-145 was not always down-regulated in patients with clinical ATL. One possible explanation may be that ATL cell line tumor cells are highly activated and more aggressive than clinical ATL cases.

We then focused on miR-145, and to confirm whether miR-145 expression was inversely associated with ATL cell proliferation, we performed an MTT assay to measure cell proliferation rates before and after enforced miR-145 expression in an ATL cell line, MT-4, and showed that overexpression of miR-145 significantly inhibited tumor cell growth. This inhibition was not complete, suggesting that some other factors or pathways may be involved in tumor cell growth. Down-regulation of miR-145 has been reported in various types of human carcinoma [17-20] and B-cell malignancy [21-23]. These studies suggest that miR-145 plays a role in controlling cell proliferation, thereby serving as a tumor suppressor. The precise upstream mechanism of miR-145 down-regulation in ATL has not been clarified.

Recently, down-regulation of miR-145 by DNA methylation and p53 mutation pathways has been suggested in prostate cancer [24]. We searched a Web site (microRNA.org-Targets and Expression; http://microrna.org/microrna) for specific targets of miR-145 and retrieved more than 20 targets with high matching scores. However, no association has been suggested between these candidate targets and ATL in the literature. Potential targets of miR-145 have been reported including MYC in colon cancer [25], ERG in prostate cancer [26], and connective tissue growth factor in glioblastoma [27].

In conclusion, we investigated ATL cell lines and clinical ATL cases for miRNA expression using miRNA arrays and quantitative RT-PCR, and we found that down-regulation of miR-145 was highly associated with a worsened clinical course in patients. An in vitro functional assay showed that miR-145 expression was inversely associated with tumor cell proliferation. To the best of our knowledge, the involvement of miR-145 in ATL has not been reported. Our findings shed light on the biological and clinical roles of miR-145 in ATL and provide the basis for the development of new miRNA-targeted therapeutic strategies against this tumor.

## Supplementary data

Supplementary data to this article can be found online at http://dx.doi.org/10.1016/j.humpath.2014.01.017.

## Acknowledgments

We thank Mr T. Sakakibara and Dr H. Takino for their valuable comments.

## References

[1] Bartel DP. MicroRNAs: genomics, biogenesis, mechanism, and function. Cell 2004;116:281-97.
[2] Kato M, Slack FJ. MicroRNAs: small molecules with big roles: *C. elegans* to human cancer. Biol Cell 2008;100:71-81.
[3] Kong YW, Ferland-McCollough D, Jackson TJ, Bushell M. microRNAs in cancer management. Lancet Oncol 2012;13:e249-58.
[4] Matsuoka M, Jeang KT. Human T-cell leukaemia virus type 1 (HTLV-1) infectivity and cellular transformation. Nat Rev Cancer 2007;7:270-80.
[5] Shimoyama M. Diagnostic criteria and classification of clinical subtypes of adult T-cell leukaemia-lymphoma: a report from the Lymphoma Study Group (1984-87). Br J Haematol 1991;79:428-37.
[6] Ohshima K, Jaffe ES, Kikuchi M. Adult T-cell leukemia/lymphoma. In: Swerdlow E, Campo NL, Harris ES, et al, editors. WHO classification of tumours of haematopoietic and lymphoid tissues. 4th ed. Lyon: IARC Press; 2008. p. 281-4.
[7] Ishida T, Ueda R. Immunopathogenesis of lymphoma: focus on CCR4. Cancer Sci 2011;102:44-50.
[8] Yeung ML, Yasunaga J, Bennasser Y, et al. Roles for microRNAs, miR-93 and miR-130b, and tumor protein 53-induced nuclear protein 1 tumor suppressor in cell growth dysregulation by human T-cell lymphotrophic virus 1. Cancer Res 2008;68:8976-85.
[9] Bellon M, Lepelletier Y, Hermine O, Nicot C. Deregulation of microRNA involved in hematopoiesis and the immune response in HTLV-1 adult T-cell leukemia. Blood 2009;113:4914-7.
[10] Pichler K, Schneider G, Grassmann R. MicroRNAs miR-146a and further oncogenesis-related cellular microRNAs are dysregulated in HTLV-1 transformed T lymphocytes. Retrovirology 2008;5:100.
[11] Yamagishi M, Nakano K, Miyake A, et al. Polycomb-mediated loss of miR-31 activates NIK-dependent NF-kB pathway in adult T cell leukemia and other cancers. Cancer Cell 2012;21:121-35.
[12] Tomita M, Tanaka Y, Mori N. MicroRNA miR-146a is induced by HTLV-1 Tax and increases the growth of HTLV-1 infected T-cells. Int J Cancer 2012;130:2300-9.
[13] Ishihara K, Sasaki D, Tsuruda K, et al. Impact of miR-155 and miR-126 as novel biomarkers on the assessment of disease progression and prognosis in adult T-cell leukemia. Cancer Epidemiol 2012;36:560-5.
[14] Baecher-Allan C, Brown JA, Freeman GJ, Hafler DA. CD4+CD25 high regulatory cells in human peripheral blood. J Immunol 2001;167:1245-53.
[15] Sakaguchi S, Miyara M, Costantino CM, Hafler DA. FOXP3+ regulatory T cells in the human immune system. Nat Rev Immunol 2010;10:490-500.
[16] Ralfkiaer U, Hagedorn RH, Bangsgaard N, et al. Diagnostic microRNA profiling in cutaneous T-cell lymphoma (CTCL). Blood 2011;118:5891-900.
[17] Sempere LF, Christensen M, Silahtaroglu A, et al. Altered microRNA expression confined to specific epithelial cell subpopulations in breast cancer. Cancer Res 2007;67:11612-20.
[18] Cho WC, Chow AS, Au JS. Restoration of tumour suppressor hsa-miR-145 inhibits cancer cell growth in lung adenocarcinoma patients with epidermal growth factor receptor mutation. Eur J Cancer 2009;45:2197-206.
[19] Zaman MS, Chen Y, Deng G, et al. The functional significance of microRNA-145 in prostate cancer. Bri J Cancer 2010;103:256-64.
[20] Gao P, Wong CC, Tung EK, Lee JM, Wong CM, Ng IO. Deregulation of microRNA expression occurs early and accumulates in early stages of HBV-associated multistep hepatocarcinogenesis. J Hepatol 2011;54:1177-84.
[21] Akao Y, Nakagawa Y, Kitada Y, Kinoshita T, Naoe T. Down-regulation of microRNAs-143 and -145 in B-cell malignancies. Cancer Sci 2007;98:1914-20.
[22] Roehle A, Hoefig KP, Repsilber D, et al. MicroRNA signatures characterize diffuse large B-cell lymphomas and follicular lymphomas. Br J Haematol 2008;142:732-44.
[23] Fischer L, Hummel M, Korfel A, Lenze D, Joehrens K, Thiel E. Differential micro-RNA expression in primary CNS and nodal diffuse large B-cell lymphomas. Neuro-Oncol 2011;13:1090-8.
[24] Suh SO, Chen Y, Zaman MS, et al. MicroRNA-145 is regulated by DNA methylation and p53 gene mutation in prostate cancer. Carcinogenesis 2011;32:772-8.
[25] Sachdeva M, Zhu S, Wu F, et al. p53 represses c-Myc through induction of the tumor suppressor miR-145. Proc Natl Acad Sci U S A 2009;106:3207-12.
[26] Hart M, Wach S, Nolte E, et al. The proto-oncogene ERG is a target of microRNA miR-145 in prostate cancer. FEBS J 2013;280:2105-16.
[27] Lee HK, Bier A, Cazacu S, et al. MicroRNA-145 is downregulated in glial tumors and regulates glioma cell migration by targeting connective tissue growth factor. PLoS One 2013;8:e54652.

VOLUME 32 · NUMBER 11 · APRIL 10 2014

JOURNAL OF CLINICAL ONCOLOGY

ORIGINAL REPORT

# Multicenter Phase II Study of Mogamulizumab (KW-0761), a Defucosylated Anti-CC Chemokine Receptor 4 Antibody, in Patients With Relapsed Peripheral T-Cell Lymphoma and Cutaneous T-Cell Lymphoma

*Michinori Ogura, Takashi Ishida, Kiyohiko Hatake, Masafumi Taniwaki, Kiyoshi Ando, Kensei Tobinai, Katsuya Fujimoto, Kazuhito Yamamoto, Toshihiro Miyamoto, Naokuni Uike, Mitsune Tanimoto, Kunihiro Tsukasaki, Kenichi Ishizawa, Junji Suzumiya, Hiroshi Inagaki, Kazuo Tamura, Shiro Akinaga, Masao Tomonaga, and Ryuzo Ueda*

Michinori Ogura, Nagoya Daini Red Cross Hospital; Takashi Ishida and Hiroshi Inagaki, Nagoya City University Graduate School of Medical Sciences; Kazuhito Yamamoto, Aichi Cancer Center; Ryuzo Ueda, Aichi Medical University School of Medicine, Nagoya; Kiyohiko Hatake, Japanese Foundation for Cancer Research; Kensei Tobinai, National Cancer Center Hospital; Shiro Akinaga, Kyowa Hakko Kirin, Tokyo; Masafumi Taniwaki, Kyoto Prefectural University of Medicine, Kyoto; Kiyoshi Ando, Tokai University School of Medicine, Kanagawa; Katsuya Fujimoto, Hokkaido University Graduate School of Medicine, Sapporo; Toshihiro Miyamoto, Kyushu University Graduate School of Medical Sciences; Naokuni Uike, National Hospital Organization Kyushu Cancer Center; Kazuo Tamura, Fukuoka University, Fukuoka; Mitsune Tanimoto, Okayama University Hospital, Okayama; Kunihiro Tsukasaki, Nagasaki University Graduate School of Biomedical Science; Masao Tomonaga, Japanese Red Cross Nagasaki Atomic Bomb Hospital, Nagasaki; Kenichi Ishizawa, Tohoku University Hospital, Sendai; and Junji Suzumiya, Shimane University Hospital, Izumo, Japan.

Published online ahead of print at www.jco.org on March 10, 2014.

Both M.O. and T.I. contributed equally to this work.

Authors' disclosures of potential conflicts of interest and author contributions are found at the end of this article.

Clinical trial information: NCT01192984.

Corresponding author: Michinori Ogura, MD, PhD, Department of Hematology and Oncology, Nagoya Daini Red Cross Hospital, 2-9 Myoken-cho, Showa-ku, Nagoya 466-8650, Japan; e-mail: mi-ogura@naa.att.ne.jp.



0732-183X/14/3211w-1157w/$20.00

DOI: 10.1200/JCO.2013.52.0924

## ABSTRACT

### Purpose
CC chemokine receptor 4 (CCR4) is expressed by peripheral T-cell lymphomas (PTCLs) and is associated with poor outcomes. Mogamulizumab (KW-0761) is a defucosylated humanized anti-CCR4 antibody engineered to exert potent antibody-dependent cellular cytotoxicity. This multicenter phase II study evaluated the efficacy and safety of mogamulizumab in patients with relapsed PTCL and cutaneous T-cell lymphoma (CTCL).

### Patients and Methods
Mogamulizumab (1.0 mg/kg) was administered intravenously once per week for 8 weeks to patients with relapsed CCR4-positive PTCL or CTCL. The primary end point was the overall response rate, and the secondary end points included safety, progression-free survival (PFS), and overall survival (OS).

### Results
A total of 38 patients were enrolled, and 37 patients received mogamulizumab. Objective responses were noted for 13 of 37 patients (35%; 95% CI, 20% to 53%), including five patients (14%) with complete response. The median PFS was 3.0 months (95% CI, 1.6 to 4.9 months), and the median OS was not calculated. The mean maximum and trough mogamulizumab concentrations (± standard deviation) after the eighth infusion were 45.9 ± 9.3 and 29.0 ± 13.3 μg/mL, respectively. The most common adverse events were hematologic events, pyrexia, and skin disorders, all of which were reversible and manageable.

### Conclusion
Mogamulizumab exhibited clinically meaningful antitumor activity in patients with relapsed PTCL and CTCL, with an acceptable toxicity profile. Further investigation of mogamulizumab for treatment of T-cell lymphoma is warranted.

*J Clin Oncol 32:1157-1163. © 2014 by American Society of Clinical Oncology*

## INTRODUCTION

Mature T/natural killer (NK)-cell neoplasms comprise approximately 20 subclassified heterogeneous groups of non-Hodgkin lymphomas (NHLs) that account for approximately 10% of NHLs in Western countries[1-3] and approximately 25% of NHLs in Japan.[4,5] Mature T/NK-cell neoplasms are largely subdivided into peripheral T-cell lymphoma (PTCL) and cutaneous T-cell lymphoma (CTCL), and different treatment strategies are used for each of these entities.[1,6]

According to the WHO classification, PTCL includes peripheral T-cell lymphoma not otherwise specified (PTCL-NOS), angioimmunoblastic T-cell lymphoma (AITL), and anaplastic large-cell lymphoma (ALCL).[1-3] Cyclophosphamide, doxorubicin, vincristine, and prednisone (CHOP) and CHOP-like regimens have been widely used as the standard first-line treatment for patients with PTCL.[7,8] With the exception of those patients with anaplastic lymphoma kinase-positive ALCL, the efficacy of these combination therapies is unsatisfactory because those who achieve remission eventually experience relapse and poor outcomes.[3,9] Several agents have been approved by the US Food and Drug Administration for the treatment of relapsed or refractory (Rel/Ref) PTCL: pralatrexate, romidepsin for Rel/Ref PTCL, and brentuximab vedotin for Rel/Ref ALCL. The overall response rates

(ORRs) were reported to be 29% and 25% for PTCL and 86% for ALCL, respectively.[10-12]

CTCL can be classified as mycosis fungoides (MF), Sézary syndrome, or cutaneous ALCL. The majority of cases of CTCL in Japan consist of MF.[13] The therapeutic approaches and outcomes for these conditions are primarily dependent on disease stage.[6,7,14] Patients with advanced stage CTCL who relapse after systemic chemotherapies and those with transformed MF have particularly poor outcomes.[15,16] Recently, the US Food and Drug Administration approved agents for Rel/Ref CTCL treatment, including vorinostat, denileukin diftitox, and romidepsin, with ORRs of 30%, 30%, and 34%, respectively.[17-19] However, there are few treatment options or approved agents for CTCL in Japan, partly because of its low prevalence here.[5,12,13]

CC chemokine receptor 4 (CCR4) is a marker for type 2 helper T cells or regulatory T (Treg) cells and is expressed on tumor cells in approximately 30% to 65% of patients with PTCL.[20,21] CCR4-positive patients (eg, in the PTCL-NOS subgroup) have a shorter survival time when compared with CCR4-negative patients.[21-23] Further, CCR4 expression increases with advancing disease stage in patients with MF/Sézary syndrome.[24]

Mogamulizumab (KW-0761) is a humanized anti-CCR4 monoclonal antibody with a defucosylated Fc region that enhances antibody-dependent cellular cytotoxicity.[25,26] In vitro antibody-dependent cellular cytotoxicity assay and in vivo studies in a humanized mouse model revealed that mogamulizumab exhibited potent antitumor activity against T-cell lymphoma cell lines and against primary CTCL cells from patients.[26-28]

In a phase I study of patients with relapsed adult T-cell leukemia-lymphoma (ATL) and PTCL/CTCL, mogamulizumab was well tolerated up to a dose of 1.0 mg/kg. An ORR of 31% (five of 16) was obtained, including one partial response (PR) among three patients with PTCL/CTCL.[29] Mogamulizumab yielded an ORR of 50% (13 of 26) for relapsed CCR4-positive ATL in a subsequent phase II study.[30] In the United States, a phase I/II study for patients with Rel/Ref CTCL revealed that mogamulizumab was well tolerated with an ORR of 37% (14 of 38, 8% complete response [CR], 29% PR) and a median PFS of 341 days.[31]

The present report describes the results of a multicenter phase II study in Japan that was designed to assess the efficacy and safety of mogamulizumab in patients with relapsed CCR4-positive PTCL or CTCL.

## PATIENTS AND METHODS

### Study Design and Treatment

This was a multicenter, single-arm phase II study conducted at 15 Japanese centers. At least 35 patients were required to detect a lower limit of the 95% CI that exceeded the 5% threshold, and the expected ORR for mogamulizumab was 25% with a statistical power of 90%.[10,29]

All patients gave written informed consent before enrollment. Patients received intravenous infusions of 1.0 mg/kg mogamulizumab once per week for 8 weeks. Dose modification of mogamulizumab was not allowed. Oral antihistamine and acetaminophen were given before each dose of mogamulizumab as premedication.[29,30] A systemic corticosteroid (hydrocortisone 100 mg intravenously) was also administered before the first dose of mogamulizumab to prevent an infusion reaction. The same dose of hydrocortisone was administered before the second and subsequent administrations at the investigators' discretion. The plasma concentrations of mogamulizumab and antimogamulizumab antibodies in plasma were determined by using enzyme-linked immunosorbent assays.[29,30] Blood samples were collected from all patients who received at least one dose of mogamulizumab at times determined by the protocol for pharmacokinetic analyses. Maximum plasma mogamulizumab concentration and trough concentration parameters were calculated from 0 to 7 days after the eight doses. T-cell subsets and NK cell distribution were also investigated by flow cytometry during and after mogamulizumab treatment. This study was conducted in accordance with the Declaration of Helsinki and in compliance with Good Clinical Practices. The protocol was approved by the institutional review board at each participating institution.

### Patients

Patients who were ≥ 20 years of age and who had CCR4-positive PTCL or CTCL with relapse after their last systemic chemotherapy were eligible for participation. Patients who were refractory to their most recent therapy were not eligible for this study. Histopathological subtypes were assessed and reclassified by the Independent Pathology Review Committee according to the 2008 WHO classification.[1] CCR4 expression was determined by immunohistochemistry by using an anti-CCR4 monoclonal antibody (KM2160) and was confirmed by central review, as described previously.[29] In brief, CCR4 expression was classified according to the proportion of stained tumor cells (negative, < 10%; 1+, 10% to <25%; 2+, 25% to < 50%; 3+, ≥ 50%). Staging of nodal/extranodal and/or cutaneous lesions was performed if the lesions met the following requirements: nodal and extranodal lesions were > 1.5 cm in measurable length on cross-sectional computed tomography images, cutaneous lesions were identifiable on visual inspection, and peripheral blood abnormal lymphocyte count was ≥ 1,000/μL and comprised ≥ 5% of total leukocytes. All patients were required to have an Eastern Cooperative Oncology Group performance status of 0 to 2. Other notable eligibility criteria regarding laboratory values were as follows: neutrophil count ≥ 1,500/μL, platelet count ≥ 50,000/μL, hemoglobin level ≥ 8.0 g/dL, AST level ≤ 2.5× the upper limit of normal (ULN), ALT level ≤ 2.5× the ULN, total bilirubin level ≤ 1.5× the ULN, and serum creatinine level ≤ 1.5× the ULN. Patients were excluded if they had any severe complications, such as CNS involvement or a bulky lymphoma mass requiring emergent radiotherapy, a history of allogeneic stem-cell transplantation, active concurrent cancers, an active infection, or positivity for hepatitis B virus DNA, hepatitis B surface antigen, hepatitis C virus antibody, or human immunodeficiency virus antibody.

### Efficacy and Safety Assessment

The primary objective was to assess the best overall response, and the secondary objectives included assessments of the best response according to disease site, progression-free survival (PFS), and overall survival (OS). Efficacy was evaluated by the Independent Efficacy Assessment Committee according to modified response criteria based on the International Working Group Criteria.[32,33] Cutaneous lesions were evaluated by using the modified Severity Weighted Assessment Tool.[34] In addition, treatment efficacy in patients with CTCL was evaluated by using a Global Response Score.[35] Responses were assessed after the fourth and eighth mogamulizumab infusions and at 2 and 4 months after the end of treatment. Treatment was discontinued if progressive disease (PD) was evident. PD and survival were monitored until at least 4 months after the completion of dosing. For safety evaluations, adverse events (AEs) were graded according to the National Cancer Institute Common Terminology Criteria for AEs, version 4.0.

### Statistical Analysis

PFS and OS were analyzed by using the Kaplan-Meier method. PFS was defined as the time from the first dose of mogamulizumab to progression, relapse, or death by any cause (whichever occurred first). OS was measured from the day of the first dose to death by any cause.

## RESULTS

### Patient Characteristics

Sixty-five patients were screened, and 64 biopsy specimens were histologically confirmed as PTCL or CTCL by the Independent Pathology Review Committee. In total, 50 (78%) of the 64 screened

  